

Mutational Analysis of *Candida albicans* SNF7 Reveals Genetically Separable Rim101 and ESCRT Functions and Demonstrates Divergence in bro1-Domain Protein Interactions

Julie M. Wolf and Dana A. Davis¹

Department of Microbiology, University of Minnesota, Minneapolis, Minnesota 55455

Manuscript received November 13, 2009

Accepted for publication December 14, 2009

ABSTRACT

The opportunistic pathogen *Candida albicans* can grow over a wide pH range, which is associated with its ability to colonize and infect distinct host niches. *C. albicans* growth in neutral-alkaline environments requires proteolytic activation of the transcription factor Rim101. Rim101 activation requires Snf7, a member of the endosomal sorting complex required for transport (ESCRT) pathway. We hypothesized that Snf7 has distinct functions in the Rim101 and ESCRT pathways, which we tested by alanine-scanning mutagenesis. While some *snf7* alleles conferred no defects, we identified alleles with solely ESCRT-dependent, solely Rim101-dependent, or both Rim101- and ESCRT-dependent defects. Thus, Snf7 function in these two pathways is at least partially separable. Both Rim101- and ESCRT-dependent functions require Snf7 recruitment to the endosomal membrane and alleles that disrupted both pathways were found to localize normally, suggesting a downstream defect. Most alleles that conferred solely Rim101-dependent defects were still able to process Rim101 normally under steady-state conditions. However, these same strains did display a kinetic defect in Rim101 processing. Several alleles with solely Rim101-dependent defects mapped to the C-terminal end of Snf7. Further analyses suggested that these mutations disrupted interactions with bro-domain proteins, Rim20 and Bro1, in overlapping but slightly divergent Snf7 domains.

CANDIDA *albicans* is a common cause of nosocomial, hematogenously disseminated systemic infection, which has an attributable mortality of up to 50% even with antifungal therapy (PERLROTH *et al.* 2007; PFALLER and DIEKEMA 2007). The success of *C. albicans* as a pathogen is principally due to its success as a human commensal. As a commensal, *C. albicans* colonizes diverse surfaces, including the oral, intestinal, or vaginal mucosa in at least 80% of the adult human population (PFALLER and DIEKEMA 2007; SOUTHERN *et al.* 2008). While *C. albicans* primarily causes non-life-threatening infections at these sites, life-threatening systemic infections can arise through escape of commensals from mucosal sites (ANDRUTIS *et al.* 2000; MAVOR *et al.* 2005). Thus, *C. albicans* must be able to thrive in diverse host environments to survive as a commensal and cause disease as a pathogen.

One environmental condition that varies markedly in sites colonized by *C. albicans* is pH. *C. albicans* can survive and thrive in the most acidic host sites, such as the stomach and vaginal cavity, and the most alkaline sites, such as the colon. *C. albicans* can grow over a wide

pH range *in vitro* (pH 2–10), demonstrating the flexibility of *C. albicans* in the face of environmental pH. The ability to adapt to distinct environmental pH is critical for survival and pathogenesis for several reasons. First, environmental pH is a potent inducer of the *C. albicans* yeast-to-hyphae transition, which is crucial for pathogenesis (DAVIS *et al.* 2000a; LIU 2001, 2002; GOW *et al.* 2002; DAVIS 2003). Second, the expression profile of gene families relevant to pathogenesis, such as the secreted aspartyl protease family, is regulated by extracellular pH (BORG-VON ZEPELIN *et al.* 1998; BENSEN *et al.* 2004). Third, environmental pH affects the kinetics of extracellular enzymes, including virulence factors (BORG-VON ZEPELIN *et al.* 1998). Fourth, environmental pH affects nutrient uptake, as many plasma membrane transporters use the proton gradient, which is not maintained at alkaline pH (KING *et al.* 2004). Nutrient solubility is also affected in neutral-alkaline environments, making their uptake more difficult (HOWARD 1999; BENSEN *et al.* 2004; BAEK *et al.* 2008). Therefore, to survive and infect the host, *C. albicans* must respond appropriately to environmental pH.

Several distinct pH-sensing systems that are required for adaptation of *C. albicans* to neutral-alkaline pH environments have been identified (PORTA *et al.* 1999; DAVIS *et al.* 2000b, 2002; DAVIS 2003, 2009; KULLAS *et al.* 2007; SHETH *et al.* 2008). One system, the Rim101 signal

Supporting information is available online at <http://www.genetics.org/cgi/content/full/genetics.109.112029/DC1>.

¹Corresponding author: Department of Microbiology, University of Minnesota, 1360 Mayo Bldg., MMC196, 420 Delaware St. SE, Minneapolis, MN 55455. E-mail: dadavis@umn.edu

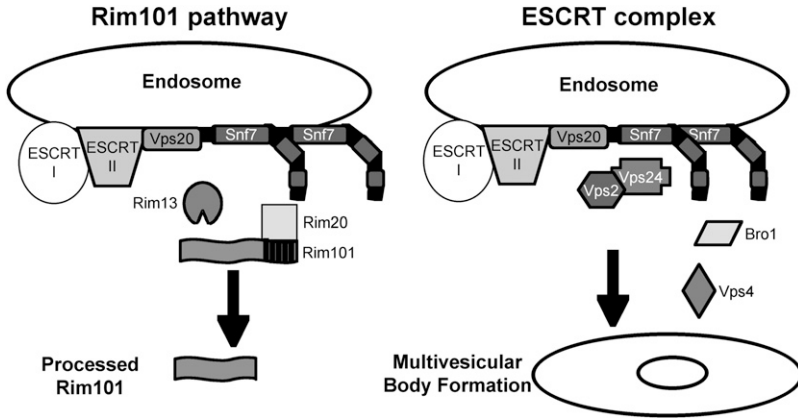


FIGURE 1.—Model of Snf7 role in Rim101 processing and in ESCRT complex functions. On the left, ESCRT-I and -II recruitment of Vps20–Snf7 to the endosomal membrane leads to Snf7 interaction with the protease Rim13 and scaffold protein Rim20. Rim20 interacts with the C-terminal PEST-like domain of Rim101, and these interactions lead to Rim101 processing to its active form. On the right, ESCRT-I and -II recruitment of Vps20–Snf7 leads to downstream recruitment of Vps2/Vps24 and Bro1. Vps4 interacts with Snf7 to facilitate ESCRT-III dissociation from the membrane, and these interactions lead to multivesicular body formation.

transduction pathway, regulates activity of the transcription factor Rim101. A similar pH-dependent Rim101/PacC pathway has been detected in a number of ascomycetes and basidiomycetes, including *Saccharomyces cerevisiae*, *Aspergillus nidulans*, and *Ustilago maydis* (LAMBERT *et al.* 1997; PENALVA and ARST 2004; ARECHIGA-CARVAJAL and RUIZ-HERRERA 2005). Rim101 is activated at neutral-alkaline pH by the proteolytic removal of an inhibitory C-terminal domain (Figure 1) (DAVIS 2003). Proteolytic activation requires upstream members, including Rim13, which acts as the putative protease (LI *et al.* 2004), and Rim20, which interacts with a PEST-like motif in the Rim101 C-terminal domain (XU and MITCHELL 2001; VINCENT *et al.* 2003). Rim101 activation also requires Snf7, which interacts with Rim13 and Rim20 (ITO *et al.* 2001; XU and MITCHELL 2001; BOWERS *et al.* 2004; BLANCHIN-ROLAND *et al.* 2008). Therefore, Snf7 is predicted to facilitate interaction between the protease Rim13 and its substrate Rim101 via Rim20. Rim101 activation is required for growth in neutral-alkaline environments and is required for *C. albicans* virulence in animal models of both systemic and mucosal disease (PORTA *et al.* 1999; RAMON *et al.* 1999; DAVIS *et al.* 2000a,b; MITCHELL *et al.* 2007; VILLAR *et al.* 2007). Thus, the sensing and adaptation to environmental pH through the Rim101 pathway is essential for *C. albicans* pathogenesis.

Another response to alkaline pH in yeast is an increased reliance on endocytosis and vacuolar acidification for nutrient acquisition (MUNN and RIEZMAN 1994; GIAEVER *et al.* 2002). Because alkaline conditions do not generate a favorable proton gradient, plasma membrane transporters are shut down and cells rely on the internal vacuolar proton gradient. In fact, endocytosis and vacuolar acidification are essential processes for fungal growth in alkaline but not acidic environments (MUNN and RIEZMAN 1994). To deliver endosomes containing extracellular material to the vacuole, cells use the endocytic sorting complex required for transport (ESCRT) pathway. This pathway consists of the cytoplasmic protein complexes, ESCRT-0, -I, and -II, that are sequentially recruited to ubiquitylated cargo proteins at endocytic vesicle membranes (Figure 1) (WILLIAMS and URBE

2007). This then recruits the ESCRT-III heterodimer Vps20–Snf7 (KATZMANN *et al.* 2001; BABST *et al.* 2002a,b; BILODEAU *et al.* 2002; KATZMANN *et al.* 2003), which initiates Snf7 oligomerization (TEIS *et al.* 2008). Vps20–Snf7 then recruits the second half of ESCRT-III, the Vps2–Vps24 heterodimer (BABST *et al.* 2002a), which recruits downstream ESCRT members, including Bro1 and Vps4. Bro1 recruits a deubiquitinase that removes ubiquitin from the cargo protein, while Vps4 is an AAA-ATPase that dissociates ESCRT-III from the endosomal membrane, promoting multivesicular body (MVB) formation and fusion with the vacuole (FUJITA *et al.* 2003; YEO *et al.* 2003). Using the ESCRT pathway, cells are able to acquire and deliver nutrients to the vacuole, where the internal proton gradient facilitates delivery of cargo nutrients to the cytoplasm of the cell (OHSUMI and ANRAKU 1981; OHSUMI and ANRAKU 1983).

ESCRT-I and -II, as well as Vps20 and Snf7, are required for Rim101 processing (XU *et al.* 2004). Although strains lacking ESCRT-I and -II do not recruit Snf7 to the endosomal membrane, Snf7 is expressed. This suggests that Snf7 must be localized to the endosomal membrane for its function in the Rim101 pathway, where it may serve as a scaffold for the Rim101 processing machinery at the membrane surface. This idea is supported by the colocalization of Rim101 pathway member Rim20 with Snf7 in a punctate pattern when cells are grown under alkaline conditions (BOYSEN and MITCHELL 2006). Thus, Snf7 localization is important for function both in the ESCRT and in the Rim101 pathways.

In addition to colocalizing, Snf7 and Rim20 interact through the yeast two-hybrid and split-ubiquitin assays (ITO *et al.* 2001; NIKKO and ANDRE 2007). Snf7–Rim20 interactions likely occur through the Rim20 bro1-domain. The bro1-domain was first identified in the ESCRT pathway member Bro1 as a Snf7-interaction domain. (KIM *et al.* 2005; MCCULLOUGH *et al.* 2008). As both Bro1 and Rim20 act as scaffold proteins, Bro1 and Rim20 have been proposed to act as adaptors, promoting downstream Snf7 function toward the ESCRT pathway or the Rim101 pathway, respectively (BOYSEN and MITCHELL 2006).

Because Snf7 is required for both ESCRT-mediated MVB formation and for Rim101 activation, we wanted to more precisely characterize the role of Snf7 in these two processes in *C. albicans*. We hypothesized that the function of Snf7 in the ESCRT and Rim101 pathways is distinct. To test this hypothesis, we generated a series of *snf7* mutant alleles and identified specific alleles whose products disrupted the ESCRT pathway, the Rim101 pathway, or both pathways. Phenotypic analyses of our alleles have revealed that Snf7 function in the ESCRT pathway is separable from Snf7 function in the Rim101 pathway. Further analyses of these alleles have uncovered a slight variation in the bro1-domain interactions at the C-terminal end of Snf7.

MATERIALS AND METHODS

Strains and plasmids: All *C. albicans* strains from this study are derived from BWP17 (WILSON *et al.* 1999) and are listed in Table 1. To generate the *SNF7* complementation plasmid pDDB426, wild-type *SNF7* sequence was amplified by the PCR from BWP17 genomic DNA using primers 5' SNF7 comp and 3' SNF7 comp (Table 2). The resulting PCR product and *NotI*/*EcoRI*-digested pDDB78 were transformed into *S. cerevisiae* to generate pDDB426 by *in vivo* recombination (MUHLRAD *et al.* 1992). Plasmid pDDB426, and all additional plasmids generated by *in vivo* recombination in *S. cerevisiae*, were recovered from *S. cerevisiae* and transformed into DH5 α *Escherichia coli* by electroporation for amplification.

To generate an epitope-tagged *SNF7* allele, the V5-His6 tag was amplified in the PCR from the pTRACER-EF plasmid (Invitrogen) using primers 5' Snf7-V5 and 3' Snf7-V5. The resulting PCR product and *HpaI*-digested pDDB426 were transformed into *S. cerevisiae* to generate pDDB427. Purified pDDB427 was digested with *NruI* and transformed into DAY534 to generate DAY980.

To generate the *snf7* alanine-scanning alleles, two overlapping PCR products were generated using plasmid pDDB427 as template. For example, *snf7-1* was amplified from pDDB427 in two PCR reactions, the first using primers 5' SNF7 comp and 3' *snf7-1*, and the second using primers 5' *snf7-1* and 3' SNF7 comp (Table 2). The two PCR products and *NotI*/*EcoRI*-digested pDDB78 were transformed into *S. cerevisiae* to generate plasmid pDDB428 by *in vivo* recombination. This approach was used to generate plasmids pDDB428–pDDB476. Purified plasmids were digested with *NruI* and transformed into *C. albicans* strain DAY534 to generate DAY981–DAY1029. The *snf7* alleles lacking the V5 epitope (*snf7-20.1*, *snf7-35.1*, *snf7-48.1*, *snf7-47.1*, and *snf7-49.1*) were generated using the same approach except pDDB426 as the template sequence to produce pDDB481, 483, 485, 494, and 495, respectively. All mutant *snf7* alleles were sequenced to ensure that only specifically engineered mutations were present.

Specific *snf7* alleles were transformed into the *vps4 Δ* / Δ background as follows. First, the *vps4 Δ* / Δ strain DAY537 (KULLAS *et al.* 2004) was plated on 5-FOA-containing YPD plates to select for loss of the *URA3* marker through homologous recombination to generate DAY1113. DAY1113 was transformed with pDDB427, 433, 441, and 446 to generate DAY1114–DAY1117.

To generate a *Ura* marker plasmid, first *C. albicans* *URA3* was amplified from pGEM-URA3 using primers pRS/pGEMT-5 and pRS/pGEMT-3 (SPREGHINI *et al.* 2003). The resulting PCR product and *Ngo*MI-linearized pRS314 (SIKORSKI and HIETER 1989) were transformed into *S. cerevisiae* to generate pDDB76 by *in vivo* recombination. Next, pDDB200 (LI *et al.* 2004) was

digested with *Pvu*II and the *RIM101*-containing fragment was purified. The purified product and *NotI*-digested pDDB76 were transformed into *S. cerevisiae* to generate pDDB477 by *in vivo* recombination (MUHLRAD *et al.* 1992). Finally, the V5 epitope sequence was amplified from pTRACER-EF in a PCR using primers *AgeI* 5' V5 and *AGEI* 3' V5 (LI *et al.* 2004) and the resulting PCR product was transformed with *AgeI*-digested pDDB477 into *S. cerevisiae* to generate pDDB478.

Specific *snf7* mutant alleles were expressed with *RIM101*-V5 as follows. First, the *snf7 Δ* / Δ strain DAY534 (KULLAS *et al.* 2004) was plated on 5-FOA-containing YPD plates to select for loss of the *URA3* marker through homologous recombination to generate DAY1126. DAY1126 was then transformed with *Bst*II-digested pDDB478 to generate DAY1127. DAY1127 was then transformed with pDDB427, 426, 437, 461, 433, 458, 471, 472, 473, 474, 475, 440, 441, 443, 455, 476, 429, 446, 481, 483, 485, 494, and 495 to generate DAY1151, DAY1128–DAY1144, DAY1148–DAY1150, DAY1213, and DAY1214, respectively.

To generate prototrophic *vps4 Δ* / Δ , *bro1 Δ* / Δ , and *rim20 Δ* / Δ mutant strains, DAY23 (DAVIS *et al.* 2000b), DAY537, and DAY653 (KULLAS *et al.* 2004) were transformed with *NruI*-cut DDB78 and selected on SC-his medium to generate DAY1153, DAY1155, and DAY1156.

Growth and filamentation assays: Strains were regularly propagated in YPD medium (2% Bacto Peptone, 1% yeast extract, 2% dextrose). To test for growth phenotypes, YPD was buffered with 150 mM HEPES to pH 9 with NaOH, or contained 150 mM lithium chloride. M199 medium (Gibco BRL) was buffered with 150 mM HEPES and pH adjusted as described in the text. Transformants were selected on synthetic medium (SC, 0.67% yeast nitrogen base with ammonium sulfate and without amino acids, 2% dextrose) supplemented as required for the auxotrophic requirements for the cells (ADAMS *et al.* 1997). To select for *Ura*- transformants, strains were streaked on synthetic complete medium containing 0.1% 5-FOA (MP Biomedicals). All media, except that selecting for *Ura*+ transformants, was supplemented with 80 μ g of uridine/ml. Solid medium contained 2% Bacto-agar.

FM 4-64 staining: Twenty-five microliters of a YPD overnight culture was inoculated into 1 ml M199 pH 8 medium and incubated at 30° for 4.5 hr. Two microliters of 16 mM FM 4-64 (Invitrogen) in DMSO was added to each tube and the cells were incubated on ice for 15 min. Cells were then washed and resuspended in 1 ml fresh M199 pH 8 medium and incubated at 30° for 90 min. Eighty microliters of cells was transferred to a tube containing 10 μ l each of 100 mM NaN₃ and 100 mM NaF. Cells were stored on ice and examined by fluorescent microscopy.

Protein preparation: Fifty microliters of YPD medium was inoculated from an overnight culture to an OD₆₀₀ 0.05–0.07 and grown to an OD₆₀₀ 0.5–0.7. Cells were washed with 1 mM phenylmethylsulphonyl fluoride (PMSF) and then resuspended in radioimmunoprecipitation assay buffer (50 mM Tris pH 8, 150 mM NaCl, 1% NP-40, 3 mM EDTA, 0.5% deoxycholate, 0.1% SDS) with protease inhibitors (1 mM PMSF, 10 mM dithiothreitol [DTT], 1 μ g/ml each of leupeptin, aprotinin, and pepstatin). Cells were lysed by glass bead disruption by vortexing four times for 2 min each. Cell debris was removed by 15 min centrifugation at 13000 \times g. Supernatants were collected and protein concentration was determined by Bradford assay (Bio-Rad).

Cell fractionation: Overnight cultures (0.6 ml) were diluted into 100 ml M199 medium at pH 4 or pH 8 and grown roughly 6 hr at 30°. Five OD₆₀₀ cells were washed in cold 10 mM NaF/10 mM NaN₃ and pelleted. Cells were resuspended in 10 mM Tris pH 7.5/100 mM EDTA/0.5% β -mercaptoethanol/10 mM NaN₃/10 mM NaF and shaken 20 min at 37°. Cells were collected and resuspended in isotonic S buffer (40 mM Tris

TABLE 1
(Continued)

Name	Genotype	Reference
DAY1015	<i>ura3::λimm434/ura3::λimm434 arg4::hisG/arg4::hisG snf7-36::HIS1::DDB462::his1::hisG/his1::hisG snf7::ARG4/snf7::URA3-dpl200</i>	This study
DAY1016	<i>ura3::λimm434/ura3::λimm434 arg4::hisG/arg4::hisG snf7-37::HIS1::DDB463::his1::hisG/his1::hisG snf7::ARG4/snf7::URA3-dpl200</i>	This study
DAY1017	<i>ura3::λimm434/ura3::λimm434 arg4::hisG/arg4::hisG snf7-38::HIS1::DDB464::his1::hisG/his1::hisG snf7::ARG4/snf7::URA3-dpl200</i>	This study
DAY1018	<i>ura3::λimm434/ura3::λimm434 arg4::hisG/arg4::hisG snf7-39::HIS1::DDB465::his1::hisG/his1::hisG snf7::ARG4/snf7::URA3-dpl200</i>	This study
DAY1019	<i>ura3::λimm434/ura3::λimm434 arg4::hisG/arg4::hisG snf7-40::HIS1::DDB466::his1::hisG/his1::hisG snf7::ARG4/snf7::URA3-dpl200</i>	This study
DAY1020	<i>ura3::λimm434/ura3::λimm434 arg4::hisG/arg4::hisG snf7-41::HIS1::DDB467::his1::hisG/his1::hisG snf7::ARG4/snf7::URA3-dpl200</i>	This study
DAY1021	<i>ura3::λimm434/ura3::λimm434 arg4::hisG/arg4::hisG snf7-42::HIS1::DDB468::his1::hisG/his1::hisG snf7::ARG4/snf7::URA3-dpl200</i>	This study
DAY1022	<i>ura3::λimm434/ura3::λimm434 arg4::hisG/arg4::hisG snf7-43::HIS1::DDB469::his1::hisG/his1::hisG snf7::ARG4/snf7::URA3-dpl200</i>	This study
DAY1023	<i>ura3::λimm434/ura3::λimm434 arg4::hisG/arg4::hisG snf7-44::HIS1::DDB470::his1::hisG/his1::hisG snf7::ARG4/snf7::URA3-dpl200</i>	This study
DAY1024	<i>ura3::λimm434/ura3::λimm434 arg4::hisG/arg4::hisG snf7-45::HIS1::DDB471::his1::hisG/his1::hisG snf7::ARG4/snf7::URA3-dpl200</i>	This study
DAY1025	<i>ura3::λimm434/ura3::λimm434 arg4::hisG/arg4::hisG snf7-46::HIS1::DDB472::his1::hisG/his1::hisG snf7::ARG4/snf7::URA3-dpl200</i>	This study
DAY1026	<i>ura3::λimm434/ura3::λimm434 arg4::hisG/arg4::hisG snf7-47::HIS1::DDB473::his1::hisG/his1::hisG snf7::ARG4/snf7::URA3-dpl200</i>	This study
DAY1027	<i>ura3::λimm434/ura3::λimm434 arg4::hisG/arg4::hisG snf7-48::HIS1::DDB474::his1::hisG/his1::hisG snf7::ARG4/snf7::URA3-dpl200</i>	This study
DAY1028	<i>ura3::λimm434/ura3::λimm434 arg4::hisG/arg4::hisG snf7-49::HIS1::DDB475::his1::hisG/his1::hisG snf7::ARG4/snf7::URA3-dpl200</i>	This study
DAY1029	<i>ura3::λimm434/ura3::λimm434 arg4::hisG/arg4::hisG snf7-50::HIS1::DDB476::his1::hisG/his1::hisG snf7::ARG4/snf7::URA3-dpl200</i>	This study
DAY1113	<i>ura3::λimm434/ura3::λimm434 arg4::hisG/arg4::hisG snf7-51::hisG/his1::hisG vps4::ARG4/vps4::dpl200</i>	This study
DAY1114	<i>ura3::λimm434/ura3::λimm434 arg4::hisG/arg4::hisG SNF7-V5::HIS1::DDB427::his1::hisG/his1::hisG vps4::ARG4/vps4::dpl200</i>	This study
DAY1115	<i>ura3::λimm434/ura3::λimm434 arg4::hisG/arg4::hisG snf7-6::HIS1::DDB433::his1::hisG/his1::hisG vps4::ARG4/vps4::dpl200</i>	This study
DAY1116	<i>ura3::λimm434/ura3::λimm434 arg4::hisG/arg4::hisG snf7-15::HIS1::DDB441::his1::hisG/his1::hisG vps4::ARG4/vps4::dpl200</i>	This study
DAY1117	<i>ura3::λimm434/ura3::λimm434 arg4::hisG/arg4::hisG snf7-20::HIS1::DDB446::his1::hisG/his1::hisG vps4::ARG4/vps4::dpl200</i>	This study
DAY1126	<i>ura3::λimm434/ura3::λimm434 arg4::hisG/arg4::hisG snf7-41::hisG/his1::hisG snf7::ARG4/snf7::dpl200</i>	This study
DAY1127	<i>RIM101-V5::URA3::DDB478::RIM101/RIM101</i>	This study
DAY1128	<i>ura3::λimm434/ura3::λimm434 arg4::hisG/arg4::hisG SNF7::HIS1::DDB426::his1::hisG/his1::hisG snf7::ARG4/snf7::dpl200</i>	This study
DAY1129	<i>ura3::λimm434/ura3::λimm434 arg4::hisG/arg4::hisG snf7-11::HIS1::DDB437::his1::hisG/his1::hisG snf7::ARG4/snf7::dpl200</i>	This study
DAY1130	<i>ura3::λimm434/ura3::λimm434 arg4::hisG/arg4::hisG snf7-35::HIS1::DDB461::his1::hisG/his1::hisG snf7::ARG4/snf7::dpl200</i>	This study
DAY1131	<i>ura3::λimm434/ura3::λimm434 arg4::hisG/arg4::hisG snf7-6::HIS1::DDB458::his1::hisG/his1::hisG snf7::ARG4/snf7::dpl200</i>	This study
DAY1132	<i>ura3::λimm434/ura3::λimm434 arg4::hisG/arg4::hisG snf7-32::HIS1::DDB458::his1::hisG/his1::hisG snf7::ARG4/snf7::dpl200</i>	This study
DAY1133	<i>ura3::λimm434/ura3::λimm434 arg4::hisG/arg4::hisG snf7-45::HIS1::DDB471::his1::hisG/his1::hisG snf7::ARG4/snf7::dpl200</i>	This study
DAY1134	<i>ura3::λimm434/ura3::λimm434 arg4::hisG/arg4::hisG snf7-46::HIS1::DDB472::his1::hisG/his1::hisG snf7::ARG4/snf7::dpl200</i>	This study
DAY1135	<i>ura3::λimm434/ura3::λimm434 arg4::hisG/arg4::hisG snf7-47::HIS1::DDB473::his1::hisG/his1::hisG snf7::ARG4/snf7::dpl200</i>	This study
DAY1136	<i>ura3::λimm434/ura3::λimm434 arg4::hisG/arg4::hisG snf7-48::HIS1::DDB474::his1::hisG/his1::hisG snf7::ARG4/snf7::dpl200</i>	This study
	<i>RIM101-V5::URA3::DDB478::RIM101/RIM101</i>	

(continued)

TABLE 1
(Continued)

Name	Genotype	Reference
DAY1137	<i>ura3::λimm434/ura3::λimm434 arg4::hisG/arg4::hisG snf7-49::HIS1::DDB475::his1::hisG/his1::hisG snf7::ARG4/snf7::dpl200</i> <i>RIM101-V5::URA3::DDB478::RIM101/RIM101</i>	This study
DAY1138	<i>ura3::λimm434/ura3::λimm434 arg4::hisG/arg4::hisG snf7-14::HIS1::DDB440::his1::hisG/his1::hisG snf7::ARG4/snf7::dpl200</i> <i>RIM101-V5::URA3::DDB478::RIM101/RIM101</i>	This study
DAY1139	<i>ura3::λimm434/ura3::λimm434 arg4::hisG/arg4::hisG snf7-15::HIS1::DDB441::his1::hisG/his1::hisG snf7::ARG4/snf7::dpl200</i> <i>RIM101-V5::URA3::DDB478::RIM101/RIM101</i>	This study
DAY1140	<i>ura3::λimm434/ura3::λimm434 arg4::hisG/arg4::hisG snf7-17::HIS1::DDB443::his1::hisG/his1::hisG snf7::ARG4/snf7::dpl200</i> <i>RIM101-V5::URA3::DDB478::RIM101/RIM101</i>	This study
DAY1141	<i>ura3::λimm434/ura3::λimm434 arg4::hisG/arg4::hisG snf7-29::HIS1::DDB455::his1::hisG/his1::hisG snf7::ARG4/snf7::dpl200</i> <i>RIM101-V5::URA3::DDB478::RIM101/RIM101</i>	This study
DAY1142	<i>ura3::λimm434/ura3::λimm434 arg4::hisG/arg4::hisG snf7-50::HIS1::DDB476::his1::hisG/his1::hisG snf7::ARG4/snf7::dpl200</i> <i>RIM101-V5::URA3::DDB478::RIM101/RIM101</i>	This study
DAY1143	<i>ura3::λimm434/ura3::λimm434 arg4::hisG/arg4::hisG snf7-2::HIS1::DDB429::his1::hisG/his1::hisG snf7::ARG4/snf7::dpl200</i> <i>RIM101-V5::URA3::DDB478::RIM101/RIM101</i>	This study
DAY1144	<i>ura3::λimm434/ura3::λimm434 arg4::hisG/arg4::hisG snf7-20::HIS1::DDB446::his1::hisG/his1::hisG snf7::ARG4/snf7::dpl200</i> <i>RIM101-V5::URA3::DDB478::RIM101/RIM101</i>	This study
DAY1145	<i>ura3::λimm434/ura3::λimm434 arg4::hisG/arg4::hisG his1::hisG/his1::hisG rim101::ARG4/rim101::dpl200</i> <i>rim101-281::URA3::pDDB479::RIM101/RIM101</i>	This study
DAY1146	<i>ura3::λimm434/ura3::λimm434 arg4::hisG/arg4::hisG his1::hisG/his1::hisG snf7::ARG4/snf7::dpl200</i> <i>rim101-281::URA3::pDDB479::RIM101/RIM101</i>	This study
DAY1147	<i>ura3::λimm434/ura3::λimm434 arg4::hisG/arg4::hisG snf7-48::HIS1::DDB474::his1::hisG/his1::hisG</i> <i>snf7::ARG4/snf7::dpl200 rim101-281::URA3::pDDB479::RIM101/RIM101</i>	This study
DAY1148	<i>ura3::λimm434/ura3::λimm434 arg4::hisG/arg4::hisG snf7-20.1::HIS1::DDB481::his1::hisG/his1::hisG snf7::ARG4/snf7::dpl200</i> <i>RIM101-V5::URA3::DDB478::RIM101/RIM101</i>	This study
DAY1149	<i>ura3::λimm434/ura3::λimm434 arg4::hisG/arg4::hisG snf7-35.1::HIS1::DDB483::his1::hisG/his1::hisG snf7::ARG4/snf7::dpl200</i> <i>RIM101-V5::URA3::DDB478::RIM101/RIM101</i>	This study
DAY1150	<i>ura3::λimm434/ura3::λimm434 arg4::hisG/arg4::hisG snf7-48.1::HIS1::DDB485::his1::hisG/his1::hisG snf7::ARG4/snf7::dpl200</i> <i>RIM101-V5::URA3::DDB478::RIM101/RIM101</i>	This study
DAY1151	<i>ura3::λimm434/ura3::λimm434 arg4::hisG/arg4::hisG SNF7-V5::HIS1::DDB427::his1::hisG/his1::hisG snf7::ARG4/snf7::dpl200</i> <i>RIM101-V5::URA3::DDB478::RIM101/RIM101</i>	This study
DAY1153	<i>ura3::λimm434/ura3::λimm434 arg4::hisG/arg4::hisG HIS1::DDB78::his1::hisG/his1::hisG rim20::ARG4/rim20::URA3</i>	This study
DAY1155	<i>ura3::λimm434/ura3::λimm434 arg4::hisG/arg4::hisG HIS1::DDB78::his1::hisG/his1::hisG ups4::ARG4/ups4::URA3-dpl200</i>	This study
DAY1156	<i>ura3::λimm434/ura3::λimm434 arg4::hisG/arg4::hisG HIS1::DDB78::his1::hisG/his1::hisG bro1::ARG4/bro1::URA3-dpl200</i>	This study
DAY1213	<i>ura3::λimm434/ura3::λimm434 arg4::hisG/arg4::hisG snf7-47.1::HIS1::DDB494::his1::hisG/his1::hisG snf7::ARG4/snf7::dpl200</i> <i>RIM101-V5::URA3::DDB478::RIM101/RIM101</i>	This study
DAY1214	<i>ura3::λimm434/ura3::λimm434 arg4::hisG/arg4::hisG snf7-49.1::HIS1::DDB495::his1::hisG/his1::hisG snf7::ARG4/snf7::dpl200</i> <i>RIM101-V5::URA3::DDB478::RIM101/RIM101</i>	This study

TABLE 2
Primers used in this study

Primer name	Sequence 5'–3'
5' Snf7-HpaI-V5	TGTATCAAGAGAAGAAGAGTTACCACAATTCCCATCTGTTGGTAAGCCTATCCCTAACC
3' Snf7-HpaI-V5	CTTCATCTTCATCTTCTTCTACTACTGGAGCTTCTTGTTATGGTGATGGTGATGATGAC
5' Snf7 comp	AAGCTCGGAATTAACCCTCACTAAAGGGAACAAAAGCTGGGCCTCATTGAGCAACTTGAG
3' Snf7 comp	ACGACGGCCAGTGAATGTAAATACGACTCACTATAGGGCGTAATCGACATTAAGGACTC
5' Snf7.1	TAGTAAACAGGCCTAGGATCGCGGGAGCTTTTTTTGGAGGAAATAGCCA
3' Snf7.1	TGGCTATTTCTCCAAAAAAGCTCCCAGCATCTAGGCCTGTTTACTA
5' Snf7.2	GGCCTAGGATGTGGGGATATGCTGCTGGAGGAAATAGCCAACAAAA
3' Snf7.2	TTTTGTTGGCTATTTCTCCAGCAGCATATCCCCACATCCTAGGCC
5' Snf7.3	ATTTTTTTGGAGGAAATAGCGCAGCAAAGAAAGATTTACCAAAGAA
3' Snf7.3	TTCTTTGGTAAATCTTTCTTTGCTGCGCTATTTCTCCAAAAAAT
5' Snf7.4	TTGGAGGAAATAGCCAACAAAGCGCGCAGCTTTACCAAAGAAGGCAATAGT
3' Snf7.4	ACTATTGCCTTCTTTGGTAAAGCTGCCGCTTGTGGCTATTTCTCCAA
5' Snf7.5	AACAAAAGAAAGATTTACCAGCGCGGCAATAGTGGAAATTGCGAGA
3' Snf7.5	TCTCGCAATTCCACTATTGCCGCGCTGGTAAATCTTTCTTTTGT
5' Snf7.6	TACCAAAGAAGGCAATAGTGGCATTGGCAGCACACATACAAACACTAAACAA
3' Snf7.6	TTGTTTAGTGTTTGTATGTGTGCTGCCAATGCCACTATTGCCTTCTTTGGTA
5' Snf7.7	CAATAGTGGAAATTCGAGAAGCCATAGCAACACTAAACAAGAAGAAGAA
3' Snf7.7	TTCTTCTTCTTGTTAGTGTGGCTATGGCTTCTCGCAATCCACTATTG
5' Snf7.8	AACACATACAAACACTAAACCGCGCGCGCAACCATTTGCAACAGCAAAAT
3' Snf7.8	ATTTGCTGTTGCAAATGGTTCCGCCCGCGCTTTAGTGTTTGTATGTGT
5' Snf7.9	ACAAGAAGAAGAACCATTTGGCAGCGGCAATGGATGACCAAGAT
3' Snf7.9	AACTGATCTTGGTCATCCATTGCCGCTGCCAAATGGTTCCTTCTTCTTGT
5' Snf7.10	AGAACCATTTGCAACAGCAAGCGGCTGCCCAAGATCAGTTGGCCAGAAA
3' Snf7.10	TTTCTGGCCAACTGATCTTGGCCAGCGGCTTGTCTGTTGCAAATGGTTCT
5' Snf7.11	TGCAACAGCAAAATGGATGACGCAGCTGCCGTTGGCCAGAAAATAGTTAG
3' Snf7.11	CTAACATATTTCTGGCCAACGCAGCTGCCGTCATCCATTTGCTGTTGCA
5' Snf7.12	ATGACCAAGATCAGTTGGCCCGCAGCAGCTGTTAGTTCAAAACAAACAAC
3' Snf7.12	GTTGTTTGTGTTTGAACATAACAGCTGCTGCCGCCAACTGATCTTGGTTCAT
5' Snf7.13	CCAGAAAATATGTTAGTTCAGCAGCAACAACCTTTAGCTAAAAGTGC
3' Snf7.13	GCATTTTAGCTAAAAGTTGTTGCTGCTGAACTAACATATTTTCTGG
5' Snf7.14	CAAAACAAACAACCTTTAGCTGCAGCTGCTTTAAAAAGAAAAAAGGG
3' Snf7.14	CCCTTTTTTCTTTTTAAAGCAGCTGCAGCTAAAAGTTGTTTGTGTTT
5' Snf7.15	CAACTTTAGCTAAAAGTGTGTCAGCAGCAAAAAAGGGGTATGAATCTAA
3' Snf7.15	TTAGATTCATACCCCTTTTTTGTGCTGCTGCAGCACTTTTAGCTAAAAGTTG
5' Snf7.16	AGTGCTTTAAAAAGAGCAGCGGGGTATGCATCTAATCTATTAATAA
3' Snf7.16	TTTTAATAGATTAGATGCATACCCCGCTGCTCTTTTTAAAGCACT
5' Snf7.17	GAATCTAATCTATTAGCAGTGGCAAACCGGATTGAACTTTGGAA
3' Snf7.17	TTCCAAAGTTTCAATCGGTTTGGCACTGCTAATAGATTAGATTC
5' Snf7.18	GTGGAACCAGATTGCAACTGCGGCAACACAATTAATT
3' Snf7.18	ACTAATTAATTGTGTTGCCGAGTTGCAATCTGGTTTTCCAC
5' Snf7.19	ACCAGATTGAAACTTTGGAAGCAGCAGCAATTAGTATCGAAGGAGCAAA
3' Snf7.19	TTTGCTCCTTCGATACTAATTGCTGCTGCTTCCAAAGTTTCAATCTGGT
5' Snf7.20	CTTTGGAACACAATTAATTGCTGCCGAGGAGCAAACTTGAACCTTGA
3' Snf7.20	TCCAAGTTCAAGTTTGTCTCTGCCGCGAGCAATTAATTGTGTTTCCAAAG
5' Snf7.21	AAGGAGCAAACTTGAACCTTGGCAACTGCCGCGAGCTATGAAACAAGGAG
3' Snf7.21	TTTGCTCCTTGTTCATAGCTGCCGAGTTGCCAAGTTCAAGTTTGTCTCCT
5' Snf7.22	ACTTGGAACACTATGAAAGCTGCCGCGCAGGAGCAAAGGCCATGAAACA
3' Snf7.22	TGTTTCATGGCCTTTGCTCCTGCTGCCGCGAGCTTTCATAGTTTCCAAAGT
5' Snf7.23	ATGAAACAAGGAGCAAAAGGCCATGAAACAAATACATGGGGAATAC
3' Snf7.23	GTATTCATGATATTGCTGCCATGGCCGCTGCTCCTTGTTCAT
5' Snf7.24	CAAAGGCCATGAAACAAATAGCTGCCGAGCAGGAGGAGGAGGAAAGTTGA
3' Snf7.24	TCAACTTTGTCTACATCGTATGCCGCGAGCTATTTGTTTCATGGCCTTTG
5' Snf7.25	CAAATACATGGGGAATACGCTGTAGCCGCGAGTTGAAGATACTATGGATG
3' Snf7.25	CATCCATAGTATCTTCAACTGCCGCTACAGCGTATTTCCCATGTATTTG
5' Snf7.26	AATACGATGTAGACAAAGTTGCAGCTACTGCCGATGAAATAAGAGAACAA
3' Snf7.26	TTGTTCTTATTTTCATCCGAGTAGCTGCAACTTTGTCTACATCGTATT
5' Snf7.27	CAAAGTTGAAGATACTATGGCTGCAATAGCAGAACAAGTAGAGTTAGCC
3' Snf7.27	GGCTAACTCTACTTGTCTGCTATTGCAGCCATAGTATCTTCAACTTTG

(continued)

TABLE 2
(Continued)

Primer name	Sequence 5'–3'
5' Snf7.28	TACTATGGATGAAATAAGAGCAGCAGTAGCGTTAGCCGATGAAATCAGT
3' Snf7.28	ACTGATTTTCATCGGCTAACGCTACTGCTGCTCTTATTTTCATCCATAGTA
5' Snf7.29	CAAGTAGAGTTAGCCGCTGCAATCAGTGCAGCTATATCGAGGCC
3' Snf7.29	GGCCCTCGATATAGCTGCACTGATTGCAGCGGCTAACTCTACTTG
5' Snf7.30	ATGAAATCAGTGAAGCTATAGCGGCGCCCGTTGGTAATGAATTTGT
3' Snf7.30	ACAAATTCATTACCAACGGGCGCCGCTATAGCTTCACTGATTTTCAT
5' Snf7.31	CTATATCGAGGCCCGTTGGTAATGAATTTGTTGATGAAGATGAATT
3' Snf7.31	AATTCATCTTCATCAACAAATGCAGCACCAACGGGCTCGATATAG
5' Snf7.32	CCGTTGGTAATGAATTTGTTGCTGCAGATGAATGGACGAGAAT
3' Snf7.32	AATTCCTTCGTTCCAATTCATCTGCAGCAACAAATTCATTACCAACGG
5' Snf7.33	GTAATGAATTTGTTGATGAACTGCATTGGACGAAGAATTGAAAAGA
3' Snf7.33	TCTTTCAATTCCTTCGTTCCAATGCAGCTTCATCAACAAATTCATTAC
5' Snf7.34	TTGTTGATGAAGATGAATTGGCCGCGCAGCATTGAAAGAGTTGGAGGCAGA
3' Snf7.34	TCTGCCCTCCAACCTTTTCAATGCTGCGGCCAATTCATCTTCATCAACAA
5' Snf7.35	AAGATGAATTGGACGAAGAAGCGGCCAGCGTTGGAGGCAGAAGCTAAAAGA
3' Snf7.35	TCTTTAGCTTCTGCCTCCAACGCTGCCGCTTCTTCGTTCCAATTCATCTT
5' Snf7.36	TGGACGAAGAATTGAAAGAGGCGGCCGCGCAGAAGCTAAAAGAACA
3' Snf7.36	TCTTGTTCCTTTAGCTTCTGCGCGCCCTCTTTCAATTCCTTCGTTCCA
5' Snf7.37	TTGAAAGAGTTGGAGGCGCAGCTGCAGCACAAGAACAAGAATCATA
3' Snf7.37	TCTATGTTCTTGTTCCTTGTGCTGCAGCTGCTGCCTCCAACCTCTTTCAA
5' Snf7.38	TGGAGGCAGAAGCTAAAGAAGCAGCAGCAGACATAGAGTGCCAGCTCA
3' Snf7.38	TGAGCTGGCACTCTATGTTCTGCTGCTGCTTCTTTAGCTTCTGCCTCCA
5' Snf7.39	AAGCTAAAGAACAAGAACAAGCAGCTGCAGTGCCAGCTCAAAGGCCAAA
3' Snf7.39	TTTGCCTTTTGAGCTGGCACTGCAGCTGCTTGTTCCTTGTTCCTTTAGCTT
5' Snf7.40	GAACATAGAGTGCCAGCTGCAGCGCCAGCACCACAACCTGTATCAAGA
3' Snf7.40	TCTTGATACAGGTTGTGGTGTGCTGCGGCTGCAGCTGGCACTCTATGTTT
5' Snf7.41	TGCCAGCTCAAAGGCCAAAAGCAGCACCTGTATCAAGAGAAGAAGA
3' Snf7.41	TCTTCTTCTCTTGATACAGGTGCTGCTTTTTGCCTTTTTGAGCTGGCA
5' Snf7.42	AGGCAAAACCACAACCTGTAGCAGCAGAAGAAGAGTTACCACAATT
3' Snf7.42	AATTGTGGTAACTCTTCTTCTGCTGCTTACAGGTTGTGGTTTTGCCT
5' Snf7.43	AACCACAACCTGTATCAAGAGCAGCAGCGTTACCACAATTCATCTGT
3' Snf7.43	ACAGATGGGAATGTGGTAAACGCTGCTGCTCTTGATACAGGTTGTGGTT
5' Snf7.44	CAAGAGAAGAAGAGTTACCAGCATTCCCATCTGTTGGTAAAGCC
3' Snf7.44	GGCTTACCACAGATGGGAATGCTGGTAACTCTTCTTCTCTTG
5' Snf7.45	ATCATCACCATCACCATAACCGCGCCAGCTCCAGTAGTAGAAGAAGA
3' Snf7.45	TCTTCTTCTACTACTGGAGCTGCCCGCTTATGGTGTGGTGTATGAT
5' Snf7.46	AAGAAAGCTCCAGTAGTAGCAGCAGCTGAAGATGAAGAAGCATTG
3' Snf7.46	TTTCAATGCTTCTTCATCTTCAGCTGCTGCTACTACTGGAGCTTTCTT
5' Snf7.47	CCAGTAGTAGAAGAAGATGCAGCTGCAGAAGCATTGAAAGCATTGCAAG
3' Snf7.47	CTTGCAATGCTTTCAATGCTTCTGCAGCTGCATCTTCTTCTACTACTGG
5' Snf7.48	GAAGAAGATGAAGATGAAGCAGCAGCGCCAGCATTGCAAGCTGAAATG
3' Snf7.48	CATTTAGCTTGAATGCTGCCGCTGCTGCTTCATCTTCATCTTCTTTC
5' Snf7.49	GAAGAAGCATTGAAAGCAGCGCCAGCTGCAATGGGATTATGATGTGTT
3' Snf7.49	AACACATCATAATCCCATTCAGCTGCCGCTGCTTTCAATGCTTCTTC
5' Snf7.50	TAATTAGTATCGAAGGAGCAAACTTGAACCTTGAAACTATGAAAGCTAT
3' Snf7.50	ATAGCTTTTCATAGTTTTCCAAGGCCGCGCTGCTCCTTCGATACTAATTA

pH 7.5/1.2 M sorbitol/0.5 mM MgCl₂/10 mM NaN₃/10 mM NaF/800 µg/ml yeast lytic enzyme [MPBio]). Spheroplasts were gently pelleted and resuspended in Lysis Buffer (50 mM Tris pH 7.5/0.2 M sorbitol/2 mM EDTA) containing 10 mM DTT and protease inhibitors (1 mM PMSF, 1 µg/ml each of leupeptin, aprotinin, and pepstatin), and homogenized with 30 dounces in a glass homogenizer. Cell debris was removed by centrifugation for 10 min at 500 × g to generate the cleared homogenate. One hundred microliters of the supernatant was removed and saved at –80° as total sample. The remainder of the supernatant was centrifuged 15 min at 13,000 × g. The supernatant was removed and stored at –80° and the pellets

were washed twice with 1 ml lysis buffer, centrifuged 15 min at 13,000 × g, and resuspended in 0.5 ml lysis buffer. A 50-µl sample from each fraction (supernatant and pellet, as well as cleared homogenate) was used for Western blot analysis.

Western blot analysis: Fifty microliters of crude protein or cell fractionation sample was separated by SDS–polyacrylamide gel electrophoresis (SDS–PAGE). Resolving gels were made to 12% or 6% polyacrylamide for Rim101 or Snf7 visualization, respectively. Gels were transferred to a nitrocellulose membrane and blots were blocked 1 hr at room temperature with 5% milk in Tris-buffered saline containing 0.05% Tween-20 (TBS-T). Blots were probed in blocking solution containing

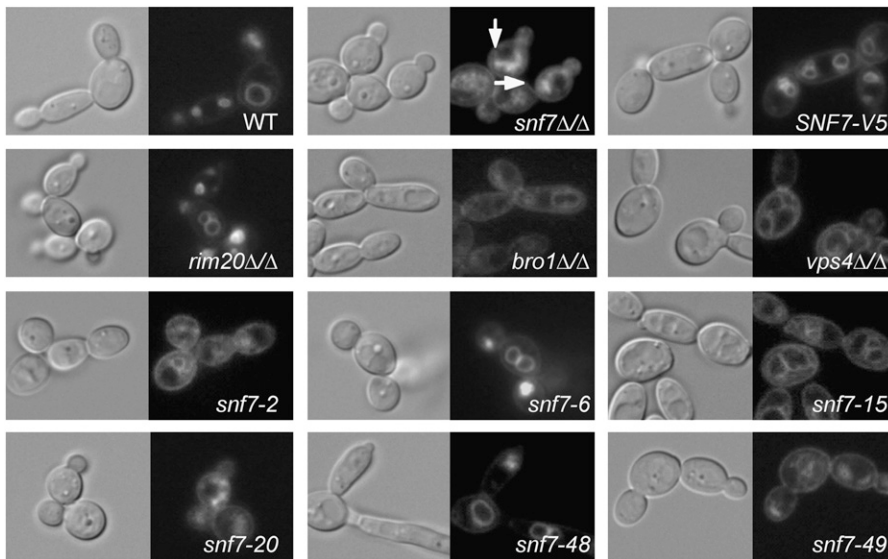


FIGURE 2.—FM 4-64 localization in *snf7* mutants, including WT (DAY185), *snf7Δ/Δ* (DAY763), *snf7Δ/Δ* + *SNF7-V5* (DAY980), *rim20Δ/Δ* (DAY1153), *bro1Δ/Δ* (DAY1156), *vps4Δ/Δ* (DAY1155), *snf7Δ/Δ* + *snf7-2* (DAY982), *snf7Δ/Δ* + *snf7-6* (DAY986), *snf7Δ/Δ* + *snf7-15* (DAY994), *snf7Δ/Δ* + *snf7-20* (DAY999), *snf7Δ/Δ* + *snf7-48* (DAY1027), and *snf7Δ/Δ* + *snf7-49* (DAY1028). Strains were grown at 30° to mid-log phase in M199 (pH 8) medium and exposed to FM 4-64 for 15 min. Cells were washed and incubated in fresh M199 pH 8 medium for 90 min at 30°. Cells were placed on ice and NaF and Na₃ were added prior to photographing. Arrows indicate Class E-like accumulations in *snf7Δ/Δ* strain.

a 1:5000 monoclonal anti-V5-HRP (Invitrogen) antibody. Blots were washed with TBS-T, incubated with ECL reagent (Amersham), and exposed to film.

Immunofluorescence: Cells were grown to mid-log phase and fixed with 4% formaldehyde for 15 min. Spheroplasts were generated using 5 μg/ml YLE (MPBio) in Solution B (100 mM potassium phosphate pH 7.5, 1.2 M sorbitol) for 15 min. Cells were pelleted at 0.5 × *g* for 5 min, washed twice in 1 ml Solution B, and spotted onto polylysine-coated slides. Samples were blocked 10 min with 5% BSA and incubated 1 hr with 1:100 anti-V5 antibody. This was followed by a 1-hr incubation with 1:200 anti-mouse IgG conjugated to alexafluor 488 (Invitrogen). Cells were visualized on a Zeiss Imager.M1 microscope and images were captured using Axiovision Release 4.6.3 software.

Filamentation assays: For filamentation assays on solid medium, 3 μl of overnight YPD cultures was spotted onto M199 pH 8 agar plates. Plates were incubated 5–7 days at 37° and photographed. For liquid filamentation assays, overnight YPD cultures were inoculated 1:100 into M199 pH 8 medium and grown for 4 hr at 37°. A total of 500 μl of cells were fixed with 1 ml ethanol for 30 min at 23°. Cell morphology was analyzed microscopically and at least 300 cells per sample were counted.

FaDu cell damage assay: FaDu cells (ATCC) were grown in 24-well tissue culture dishes and incubated at 37° 5% CO₂ in modified eagle medium (MEM) with 10% final concentration FBS and 5 ml antibiotic/antimycotic cocktail (Invitrogen). At 90% monolayer confluence, FaDu cells were incubated in 0.5 ml medium containing 0.5 μCi ⁵¹Cr for 16 hr. After washing FaDu with PBS, 1 × 10⁵ *C. albicans* cells were added in MEM with 10% FBS and 5 ml antibiotic cocktail and incubated 10 hr. Some FaDu were untreated to measure spontaneous ⁵¹Cr release. After incubation, 0.5 ml supernatant was moved to a 13-ml glass (supernatant) tube. One-half milliliter of 6 M NaOH was added to FaDu and moved to a separate (debris) tube. Final monolayer was removed to the debris tube in 0.5 ml Liftaway (RPI Corp). Specific release was calculated as [(2 × supernatant) – (2 × spontaneous release)] / [(2 × total) – (2 × spontaneous release)].

RESULTS

To determine how Snf7 functions in the Rim101 and vacuolar transport pathways, we first generated a V5

epitope-tagged *SNF7* allele. Since C-terminal Snf7-V5 fusions were not functional (data not shown), we used the internal *Hpa*I site to generate an in-frame fusion. This *SNF7-V5* allele fully complemented the endocytosis and growth defects observed in the *snf7Δ/Δ* strain (Figures 2 and 3, Table 4), demonstrating that Snf7-V5 is functional.

We predicted that distinct domains of Snf7 contribute to vacuolar transport and Rim101 activation. To address this hypothesis, we used alanine-scanning mutagenesis to generate a series of mutant *snf7-V5* alleles. Alanine residues were substituted at up to three charged residues within a span of five amino acids. Using this approach, 49 alleles were generated in the *SNF7-V5* background that span the length of the 226 residues of Snf7 protein (Table 3). To determine if these alleles affect Snf7 function in the vacuolar transport pathway, Rim101 pathway, or both pathways, the alleles were transformed into a *snf7Δ/Δ* mutant and tested for complementation of vacuolar transport and Rim101 processing defects (referred to as ESCRT-dependent and Rim101-dependent phenotypes below, although we recognize that Rim101-dependent phenotypes also depend on upstream ESCRT function).

To determine if a given mutation affected Snf7 protein stability, we performed Western blot analysis on crude protein extracts from our mutant strains. All strains containing an alanine-scanning allele produced abundant Snf7 protein (Figure 4). However, we noted that specific alleles revealed differences in mobility, such as *snf7-29*, *snf7-40*, and *snf7-47*. These differences are likely due to alterations of SDS binding; however, we cannot rule out the possibility that the altered mobilities are due to disruption of an as-yet-unknown Snf7 post-translational modification. Regardless, these results indicate that the alanine-scanning alleles are expressed and that phenotypes observed in the mutant alleles are not due to the instability of the Snf7 protein.

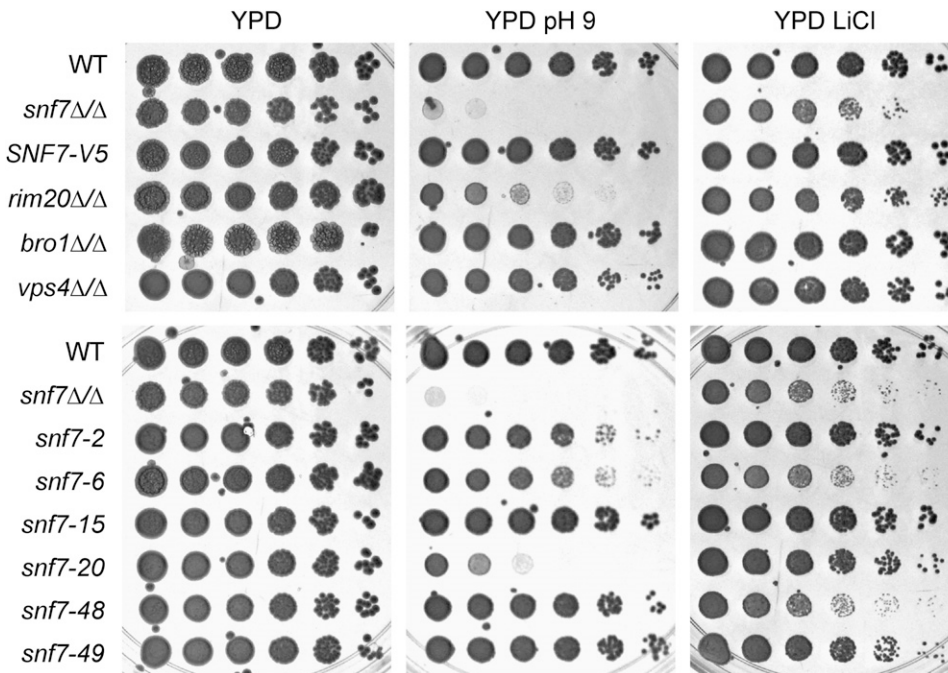


FIGURE 3.—Growth phenotypes of *snf7* mutants. Strains pictured include the wild type (WT) (DAY185), *snf7Δ/Δ* (DAY763), *snf7Δ/Δ* + *SNF7-V5* (DAY980), *rim20Δ/Δ* (DAY1153), *bro1Δ/Δ* (DAY1156), *vps4Δ/Δ* (DAY1155), *snf7Δ/Δ* + *snf7-2* (DAY982), *snf7Δ/Δ* + *snf7-6* (DAY986), *snf7Δ/Δ* + *snf7-15* (DAY994), *snf7Δ/Δ* + *snf7-20* (DAY999), *snf7Δ/Δ* + *snf7-48* (DAY1027), and *snf7Δ/Δ* + *snf7-49* (DAY1028). Strains were grown on YPD, YPD pH 9, and YPD + LiCl for 2 days at 37° prior to photographing.

When grown on rich YPD medium, the wild-type strain and the *snf7Δ/Δ* + *SNF7-V5* strain grew comparably (Figure 3). However, the *snf7Δ/Δ* mutant grew more slowly, as reported previously (KULLAS *et al.* 2004). All of the *snf7Δ/Δ* + *snf7* alanine-scanning allele strains rescued this growth defect on rich medium. This result, and the fact that Snf7 protein is expressed at similar levels in all strains, suggests that none of the *snf7* alleles is a true null.

***snf7* alleles affecting vacuolar transport:** We first analyzed the *snf7* alleles for ESCRT-dependent phenotypes. Endocytosis is required to move plasma membrane components to the vacuole and can be monitored using the fluorescent lipophilic dye, FM 4-64 (VIDA and EMR 1995). In wild-type and *snf7Δ/Δ* + *SNF7-V5* cells, FM 4-64 associated with the plasma membrane was taken up by endocytosis and was ultimately localized to the vacuolar membrane, resulting in the ring-like pattern around the vacuole (Figure 2). In *snf7Δ/Δ* cells, FM 4-64 associated with the plasma membrane and was taken up by endocytosis, but was unable to localize to the vacuole, resulting in a more diffuse staining pattern and the apparent formation of class E-like exclusion bodies around the perimeter of the vacuole (Figure 2). These exclusion bodies likely consist of endosomes unable to fully mature to MVBs and thus unable to efficiently fuse with the vacuole (KRANZ *et al.* 2001). We next tested a *rim20Δ/Δ* mutant, which does not process Rim101 but has no detected role in MVB formation (DAVIS *et al.* 2000a; KULLAS *et al.* 2004). This strain localized FM 4-64 to the vacuole like wild-type, as previously reported. We also tested a *bro1Δ/Δ* strain, which affects MVB formation but has no detected role in Rim101 processing (KULLAS *et al.* 2004 and data not shown). The *bro1Δ/Δ*

mutant showed stronger vacuolar staining than the *snf7Δ/Δ* mutant but similarly displayed class E-like bodies around the periphery of the vacuole and cytoplasmic punctate spots not observed in wild-type

TABLE 3

Snf7 mutant sequences

Allele	WT sequence ^a	Allele	WT sequence
<i>snf7-1</i>	1-MWGYF	<i>snf7-26</i>	125-VEDTM
<i>snf7-2</i>	3-GYFFG	<i>snf7-27</i>	129-MDEIR
<i>snf7-3</i>	10-SQOKK	<i>snf7-28</i>	133-REQVE
<i>snf7-4</i>	12-QKKDL	<i>snf7-29</i>	140-DEISE
<i>snf7-5</i>	17-PKKAI	<i>snf7-30</i>	146-ISRVPV
<i>snf7-6</i>	22-VELRE	<i>snf7-31</i>	151-GNEFV
<i>snf7-8</i>	32-NKKKN	<i>snf7-32</i>	155-VDEDE
<i>snf7-9</i>	38-LQQQM	<i>snf7-33</i>	157-EDELD
<i>snf7-10</i>	41-QMDDQ	<i>snf7-34</i>	160-LDEEL
<i>snf7-11</i>	44-DQDQL	<i>snf7-35</i>	163-ELKEL
<i>snf7-12</i>	49-ARKYV	<i>snf7-36</i>	166-ELEAE
<i>snf7-13</i>	55-SKOTT	<i>snf7-37</i>	169-AEAKE
<i>snf7-14</i>	61-AKSAL	<i>snf7-38</i>	173-EQEQE
<i>snf7-15</i>	64-ALKRK	<i>snf7-39</i>	176-QEHRV
<i>snf7-16</i>	68-KKGYE	<i>snf7-40</i>	182-AQKAK
<i>snf7-17</i>	77-KVENQ	<i>snf7-41</i>	186-KPQPV
<i>snf7-18</i>	82-IETLE	<i>snf7-42</i>	190-VSREE
<i>snf7-19</i>	86-ETQLI	<i>snf7-43</i>	192-REEEL
<i>snf7-20</i>	90-ISIEG	<i>snf7-44</i>	196-LPQFP
<i>snf7-50</i>	95-ANLNL	<i>snf7-45</i>	202-VNKA
<i>snf7-21</i>	100-ETMKA	<i>snf7-46</i>	209-VEEKE
<i>snf7-22</i>	105-AMKQG	<i>snf7-47</i>	212-DEDEF
<i>snf7-23</i>	111-KAMKQ	<i>snf7-48</i>	215-EEALK
<i>snf7-24</i>	116-IHGEY	<i>snf7-49</i>	220-ALQAE
<i>snf7-25</i>	120-YDVVK		

^aThe number represents the N-terminal Snf7 residue. Underlined residues are changes to alanine in the mutant.

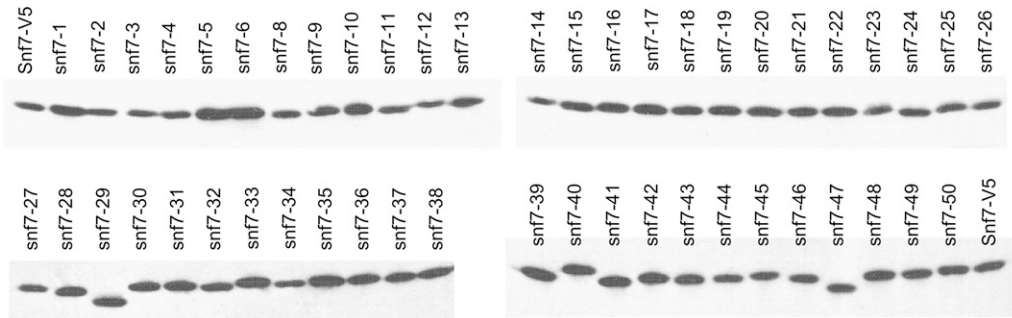


FIGURE 4.—Mutant *snf7* alleles produce detectable protein. A total of 250 μ g protein collected from mid-log cultures was loaded for each sample and run on 10% SDS-PAGE. Blots were probed with anti-V5-HRP antibody. Protein loading was normalized to anti-tubulin signal (data not shown).

cells (Figure 2). This suggests that *bro1* Δ/Δ mutants have a defect in vacuolar trafficking, but that this defect is not as severe as the *snf7* Δ/Δ mutant, as previously described in *C. albicans* and homologous *S. cerevisiae* mutants (ODORIZZI *et al.* 2003; KULLAS *et al.* 2004). Finally, we tested a *vps4* Δ/Δ strain, which also had a defect in vacuolar trafficking that was less pronounced than the *snf7* Δ/Δ mutant defect, as reported previously (KULLAS *et al.* 2004). Thus Snf7 and downstream ESCRT proteins, but not Rim101 pathway members, are required for FM 4-64 localization to the vacuole.

The *snf7* Δ/Δ + *snf7* alanine-scanning alleles were assayed for FM 4-64 localization and characterized as nonfunctional, partially functional, or fully functional. Nonfunctional alleles were defined as those that have a staining pattern that mimics the *snf7* Δ/Δ strain, such as *snf7-2* and *snf7-20* (Figure 2). Partially functional alleles were those that showed some vacuolar staining but variously retained FM 4-64 in the cytoplasm or had slightly aberrant vacuolar staining patterns, such as *snf7-15* and *snf7-49*. We noted similar patterns between some partially functional alleles, such as *snf7-15*, and the

vps4 Δ/Δ strain, which had a less severe FM 4-64 trafficking defect than the *snf7* Δ/Δ mutant (Figure 2). Fully functional alleles were defined as those that localized FM 4-64 to the vacuole similar to the *snf7* Δ/Δ + *SNF7-V5* strain, such as *snf7-6* and *snf7-48*. Thus, we were able to test the ESCRT-dependent function of our *snf7* alleles and identified several alleles from each of three categories among our *snf7* alleles (Figure 5).

***snf7* alleles affecting the Rim101 pathway:** We next analyzed the alanine-scanning *snf7* alleles for Rim101-dependent phenotypes with fivefold serial dilution growth assays. Rim101 activation is required for growth on YPD buffered to pH 9 and on YPD containing lithium chloride (LiCl) (Figure 3). These growth defects are also observed on streaked agar plates (supporting information, Figure S1). On YPD pH 9 medium, the wild-type and *snf7* Δ/Δ + *SNF7-V5* strains grew similarly, but the *snf7* Δ/Δ strain did not produce isolated colonies (Figure 3). The *rim20* Δ/Δ mutant also displayed a growth defect, although not as severe as the *snf7* Δ/Δ strain. Both the *bro1* Δ/Δ and *vps4* Δ/Δ mutant strains were able to form wild-type-sized colonies on this alkaline medium

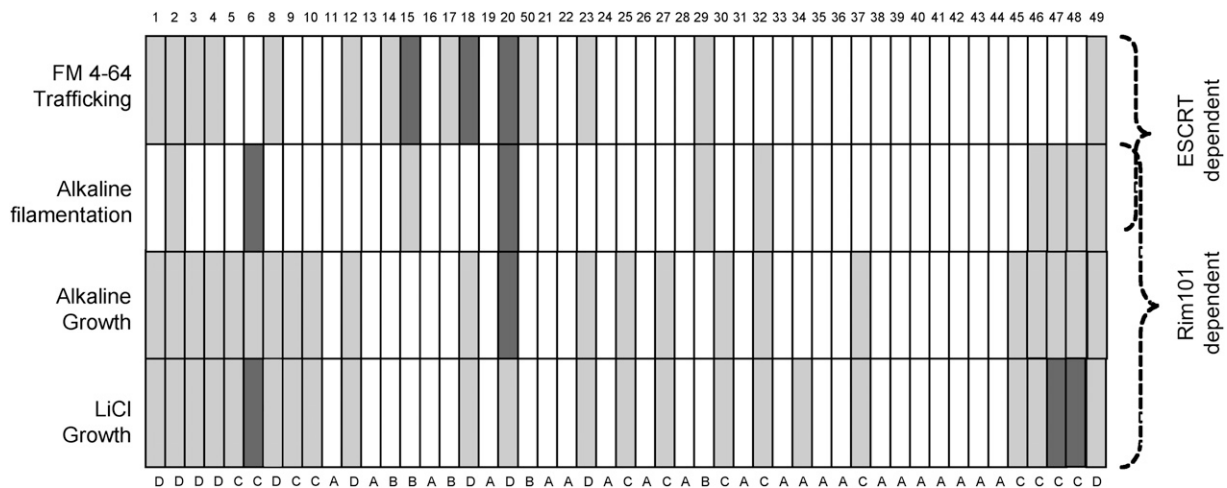


FIGURE 5.—Comparison of mutant *snf7* alleles facilitates categorization into functional groups. The cartoon represents the N- to C-terminal sequence of Snf7, with the alleles placed in order along the protein sequence. Assays are listed to the left of each row while *snf7* mutant allele number is listed above each column. Rim101- and ESCRT-dependent assays are labeled to the right side. Open blocks indicate that the mutant *snf7* allele behaves like wild-type *SNF7*, dark shaded blocks indicate that the mutant allele behaves like *snf7* Δ/Δ , and light shaded blocks indicate an intermediate phenotype. For FM 4-64 trafficking, the output is specific vacuolar staining. For alkaline filamentation, the output is percentage germ tube formation. For alkaline and LiCl growth assays, the output is colony size.

(Figure 3). Thus, *Snf7* and downstream Rim101 pathway members are required for alkaline growth, and downstream ESCRT pathway members are not.

The *snf7* Δ/Δ + *snf7* alanine-scanning alleles showed a range of growth phenotypes on alkaline medium that were categorized as nonfunctional, partially functional, or fully functional. Nonfunctional alleles were defined as those that, like the *snf7* Δ/Δ mutant, were unable to form individual colonies after 2 days growth, such as *snf7-20* (Figure 3). Partially functional alleles were defined as those that could form isolated colonies smaller than the colonies produced by the *snf7* Δ/Δ + *SNF7-V5* strain, such as *snf7-2* and *snf7-6*, and, to a lesser degree, *snf7-48* and *snf7-49* (Figure 3 and Supplemental Figure 1). Fully functional alleles were defined as those that could form isolated colonies similar in size to those produced by the *snf7* Δ/Δ + *SNF7-V5* strain, such as *snf7-15*. We identified several alleles from all three categories among our *snf7* alleles using this Rim101-dependent growth assay (Figure 5).

We next assayed growth on LiCl medium. On LiCl medium, the wild-type and *snf7* Δ/Δ + *SNF7-V5* strains grew similarly and the *snf7* Δ/Δ mutant had a severe defect, forming only pinprick-sized colonies (Figure 3). The *rim20* Δ/Δ mutant strain showed a slightly less severe growth defect, forming only very small colonies, while the *bro1* Δ/Δ and *vps4* Δ/Δ mutant strains showed no growth defects on LiCl medium (Figure 3). Thus, *Snf7* and downstream Rim101 pathway members, but not downstream ESCRT members, are required for LiCl growth.

The *snf7* Δ/Δ + *snf7* alanine-scanning alleles again showed a range of growth phenotypes on LiCl medium that were categorized as nonfunctional, partially functional, or fully functional. Nonfunctional alleles were defined as those whose colonies grew similarly to the *snf7* Δ/Δ mutant, such as *snf7-6* and *snf7-48*. Partially functional alleles were defined as those that promoted colony growth of a size intermediate between the *snf7* Δ/Δ + *SNF7-V5* and the *snf7* Δ/Δ strains, such as *snf7-2*, *snf7-20* and *snf7-49* (Figure 3). Fully functional alleles were defined as those that grew similarly to the *snf7* Δ/Δ + *SNF7-V5* strain, such as *snf7-15*. Again, we identified several alleles from all three categories among our *snf7* alleles using this assay (Figure 5).

While most *snf7* alanine-scanning alleles conferred similar growth defects on both pH 9 medium and LiCl medium (Figure 5), we did note that certain alleles showed variation between these two assays. For example, *snf7-48* was scored as partially functional on pH 9 medium but as nonfunctional on LiCl medium (Figures 3 and 5). However, no allele was fully functional in one growth assay and nonfunctional in the other. Thus, we infer that the few observed differences between these two growth assays reflect sensitivities between the growth assays. Alleles that conferred clear growth defects on both pH 9 and LiCl media were candidates for Rim101 pathway disruption.

TABLE 4
Filamentation Assay

Strain	Genotype	Alkaline agar filamentation	Acidic agar filamentation	% germ tubes ^a
DAY185	WT	+	–	96 ± 3
DAY763	<i>snf7</i> Δ/Δ	–	+	0 ± 0
DAY980	<i>SNF7-V5</i>	+	–	96 ± 1
DAY25	<i>rim101</i> Δ/Δ	–	–	0 ± 0
DAY537	<i>vps4</i> Δ/Δ	±	+	82 ± 2
DAY982	<i>snf7-2</i>	+	–	2 ± 2
DAY986	<i>snf7-6</i>	–	–	1 ± 1
DAY994	<i>snf7-15</i>	+	–	78 ± 4
DAY999	<i>snf7-20</i>	–	–	13 ± 7
DAY1028	<i>snf7-48</i>	+	–	86 ± 6

^aPercentage germ tube formation ± standard deviation from two independent experiments.

We noted that some alleles displayed both ESCRT-dependent defects and Rim101-dependent defects, such as *snf7-20*, while some alleles displayed ESCRT-dependent defects yet showed no detectable Rim101-dependent defects, such as *snf7-15*. Conversely, some alleles showing no ESCRT-dependent defects conferred Rim101-dependent defects, such as *snf7-6* and *snf7-48* (Figure 5). Thus, among these *snf7* alleles, we have identified candidate alleles with differential ESCRT- and Rim101-dependent phenotypes that are strong candidates for separation of function.

Filamentation-related *snf7* phenotypes: Vesicle trafficking and Rim101 activation are both required for filamentation, a critical virulence trait of *C. albicans* (BRUCKMANN *et al.* 2000; KULLAS *et al.* 2004; PALMER *et al.* 2005; BERNARDO *et al.* 2008). We wished to further investigate the role of these processes and their relative contributions to filamentation. Since *Snf7* is required for both ESCRT trafficking and Rim101 processing, we predicted that *snf7* alanine-scanning alleles defective in either ESCRT function or Rim101 activation would show defects in filamentation. To test this possibility, we assayed the *snf7* alanine-scanning alleles for filamentation in liquid and solid M199 pH 8 medium.

We first assessed filamentation using a quantitative liquid assay. Strains were incubated 4 hr in M199 pH 8 medium and germ tube formation was assessed for each strain. The wild-type strain produced ~95% germ tubes (Table 4). The *snf7* Δ/Δ mutant produced <0.01% germ tubes under these conditions, while the complemented *snf7* Δ/Δ + *SNF7-V5* strain rescued germ tube production. The *rim101* Δ/Δ and *rim20* Δ/Δ mutant strains were both severely deficient in germ tube production, with no detectable germ tubes after a 4-hr incubation (Table 4). The *bro1* Δ/Δ strain produced wild-type levels of germ tubes, while the *vps4* Δ/Δ strain produced ~80% germ tubes. Nonfunctional alleles were those that produced <5% germ tubes, such as *snf7-6*. Partially functional alleles were those that produced an intermediate number,

5–90%, of germ tubes, such as *snf7-15* and *snf7-48* with 78 and 88% germ tubes, respectively. Fully functional alleles were defined as those that formed >90% germ tubes like the *snf7Δ/Δ* + *SNF7-V5*. We noted that some alleles with filamentation defects also conferred ESCRT-dependent defects, such as *snf7-15*; that some also conferred Rim101-dependent defects, such as *snf7-48*; and that some also conferred defects in both, such as *snf7-20*. We did not find any alleles conferring solely filamentation defects. Although both Rim101- and ESCRT-related defects are reported to affect filamentation, we noted fewer phenotypic defects in this assay than in the FM 4-64 assay or growth assays (Figure 5).

We also assessed colony filamentation by spotting strains on solid alkaline or acidic medium and measuring the ability of the strains to form peripheral filamentation. On alkaline medium, the wild-type and *snf7Δ/Δ* + *SNF7-V5* strains formed peripheral filamentous rings (Table 4). The *snf7Δ/Δ*, *rim20Δ/Δ*, and *rim101Δ/Δ* mutants did not produce a ring of peripheral filaments, as expected due to the inability of these strains to process Rim101. The *bro1Δ/Δ* strain produced a wild-type filamentation pattern, and the *vps4Δ/Δ* mutant produced an erratic ring of peripheral filaments, as previously reported (KULLAS *et al.* 2004). The *snf7Δ/Δ* + *snf7* alanine-scanning alleles were assayed and categorized as functional or nonfunctional, as no intermediate phenotypes were observed. Nonfunctional alleles were defined as alleles that did not produce peripheral filaments, such as *snf7-6* and *snf7-20*. Fully functional alleles produced filamentous rings similar to those observed in the *snf7Δ/Δ* + *SNF7-V5* strain, such as *snf7-2*, *snf7-15*, and *snf7-48*.

On acidic solid medium, neither the wild-type, *snf7Δ/Δ* + *SNF7-V5*, *rim101Δ/Δ*, *rim20Δ/Δ*, nor the *bro1Δ/Δ* strains formed peripheral filaments (Table 4). However, we noted that both the *snf7Δ/Δ* and *vps4Δ/Δ* strains formed robust filaments. None of the mutant *snf7* alanine alleles promoted acidic filamentation, supporting our previous premise that no *snf7* mutation results in completely abolished Snf7 function. Because both Snf7 and Vps4 are required for ESCRT function and Rim101 plays no role in ESCRT function (KULLAS *et al.* 2004), our data suggest that vacuolar transport influences filamentation at acidic pH.

To define regions that may function specifically in either the ESCRT or Rim101 pathways, we mapped the results of the phenotypic assays in relation to the position of *snf7* alanine-scanning alleles (Figure 5). Alleles were classified into categories on the basis of their phenotypic profile. These included alleles that showed either no phenotypic defects or a mild defect in a single Rim101-dependent assay (group A), alleles that showed only ESCRT-dependent defects (group B), alleles that showed only Rim101-dependent defects (group C), and alleles that showed both ESCRT- and Rim101-dependent defects (group D). We then used

these groups as a guide for investigating the mechanisms behind our alanine-scanning *snf7* allele phenotypes.

Snf7 protein localization: In wild-type cells, Snf7 cycles between the cytoplasm and endosomal membrane, and its release requires Vps4. We tested Snf7 localization using cell fractionations to separate the membrane-bound organelles, including endosomes, from the cytoplasm. We first used plasma membrane protein Pma1 and cytoplasmic protein Pgk1, which localized to the pellet or supernatant fraction, respectively (data not shown), as control proteins for our fractionation protocol. Snf7-V5 was observed in both pellet and supernatant (Figure 6A), indicating that Snf7-V5 is able to cycle on and off endosomal membranes, as reported in *S. cerevisiae* (BABST *et al.* 1998). Snf7-V5 localization in a *vps4Δ/Δ* background resulted in a strong pellet signal but no supernatant signal, indicating that Snf7-V5 is unable to dissociate from endosomal membranes in the absence of Vps4, also as reported in *S. cerevisiae* (BABST *et al.* 1998). This inability to dissociate is independent of extracellular pH (data not shown). We further confirmed a Vps4-dependent Snf7 release from endosomes using immunofluorescence. Snf7-V5 fluorescence in a wild-type background showed staining throughout the cytoplasm as well as concentrated spots, which likely represent foci of Snf7 endosomal recruitment (Figure 6B). Snf7-V5 fluorescence in a *vps4Δ/Δ* background showed little cytoplasmic staining and 1 or 2 very highly concentrated spots, which likely are class E-like compartments. These two methods confirm that Snf7 localization is regulated similarly to previously described systems.

We identified 17 group D *snf7* alleles that affected Snf7 function in both the Rim101 and ESCRT pathways. Two simple models can explain the group D phenotypes. In the first model, group D alleles are defective in overall Snf7 function due to a failure of Snf7 protein to interact with the upstream ESCRT pathway member Vps20 or with Snf7 itself. Vps20 has been shown to facilitate initial Snf7 endosomal association, followed by the formation of a Snf7 lattice through Snf7-Snf7 interactions (BABST *et al.* 2002a; TEIS *et al.* 2008). Thus, *snf7* alleles unable to interact with either Vps20 or itself would not be able to properly localize, and would be expected to have a defective phenotype in any assay for Snf7 function. In the second model, group D alleles are defective in overall Snf7 function due to disruption of a Snf7 region required for interaction with downstream components of both pathways. For example, Snf7 interacts with Bro1 and Rim20 via a bro1-domain found in both proteins (VINCENT *et al.* 2003; KIM *et al.* 2005). To distinguish between these two possible explanations, Snf7 protein from the group D alleles was localized through cell fractionations.

We predicted that if group D alleles affected upstream Snf7 interactions, Snf7 protein would not be properly recruited to the endosomal membrane. To test this, we

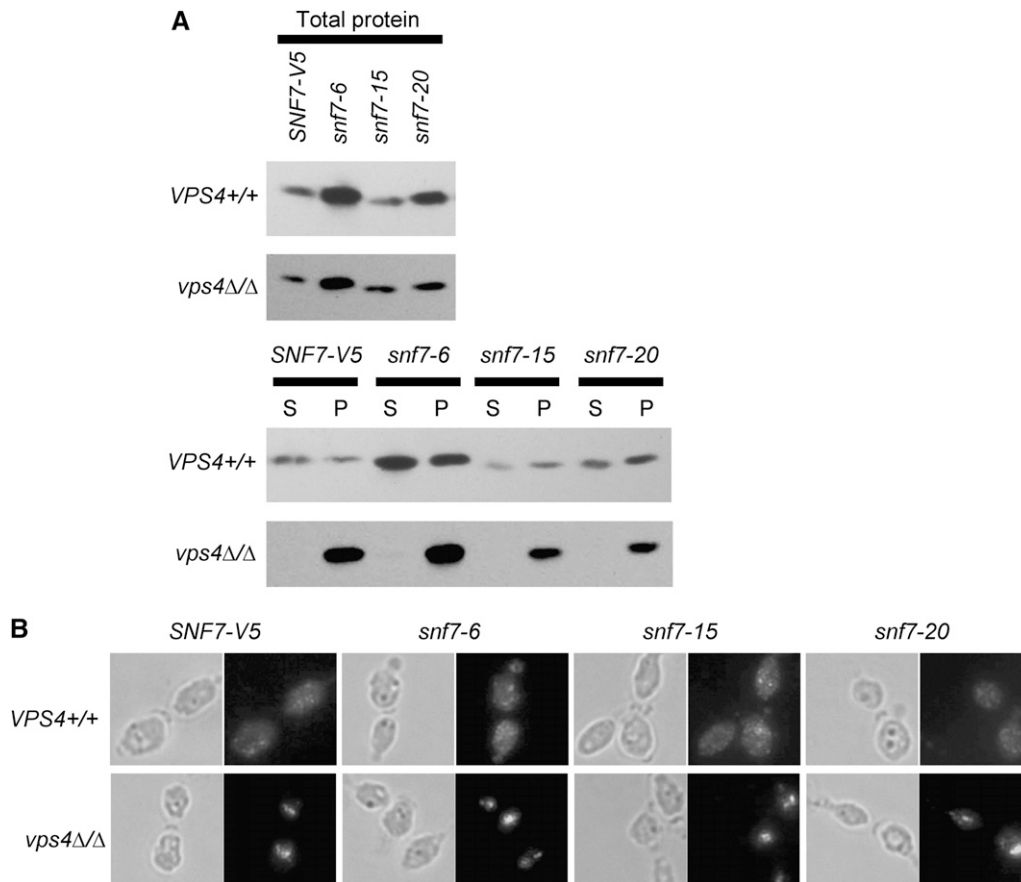


FIGURE 6.—(A) Snf7 localization remains normal in alanine-scanning *snf7* mutants during cell fractionation. Mid-log cultures were gently lysed and separated by centrifugation to generate a cytoplasm-containing supernatant (S) and an organelle-containing pellet (P). Fifty microliters of each fraction was run on 10% SDS-PAGES. Blots were probed with anti-V5-HRP antibody. (B) Snf7 localization remains normal in alanine-scanning *snf7* mutants during immunofluorescence. Strains were grown to mid-log phase in M199 (pH 8) medium, fixed with 4% formaldehyde, spheroplasted, and attached to polylysine-treated wells for immunofluorescence. Samples were treated with anti-V5 antibody, followed by anti-mouse-IgG-alexafuor 488 (green).

introduced the group D alleles into a *vps4Δ/Δ* strain, in which Snf7 protein is unable to dissociate from the endosomal membrane. If the group D allele blocked recruitment to the endosome, Snf7 should be detected only in the supernatant fraction. If the group D allele blocked downstream interactions with members of both pathways, Snf7 should be enriched in the pellet fraction. Strains containing *snf7-20* showed primarily pellet-associated Snf7 (Figure 6A), indicating that normal recruitment and retention of Snf7 in a *vps4Δ/Δ* background was retained. Results for the other group D strains were similar to *snf7-20* (data not shown). We used immunofluorescence to confirm that *snf7-20* expression leads to normal Snf7 protein localization in both a VPS4+/+ and *vps4Δ/Δ* background (Figure 6B). This suggests the mutations in these alleles affect an epitope necessary for downstream Snf7 function in both the Rim101 and ESCRT pathway.

We identified five group B alleles that affected only ESCRT-dependent Snf7 function. Because Rim101 function requires endosomal Snf7 localization, and because these alleles did not affect Rim101 function, we predicted that alleles in this category affected interactions with downstream ESCRT pathway members, such as Vps2, Vps24, or Vps4. Because we had noted a similar FM 4-64 staining pattern between the *snf7-15* and *vps4Δ/Δ* strains (Figure 2), we considered *snf7-15* to be

a strong candidate for interrupted Snf7-Vps4 interactions. To test this possibility, we investigated Snf7-15 localization by cell fractionation. Alanine scanning alleles affecting Snf7-Vps4 interactions should have enriched Snf7 protein in the pellet fraction, as the *vps4Δ/Δ* strain does, while mutant alleles not affecting Snf7-Vps4 interactions should have Snf7 in both the pellet and supernatant fractions, as the wild-type strain (Figure 6A). Snf7-15 protein was found in both pellet and cytoplasmic fractions, suggesting that Snf7-Vps4 interactions are not inhibited in this strain. We expected group C alleles, which conferred only Rim101-dependent defect, would promote Snf7 protein localization similar to wild-type and we detected both pellet- and supernatant-associated Snf7 protein in all group C alleles, such as *snf7-6* (Figure 6A). Normally regulated Snf7 protein localization from both the *snf7-6* and *snf7-15* alleles was confirmed with immunofluorescence (Figure 6B). Thus, we did not find any *snf7* alleles that significantly affected protein localization patterns.

Rim101 processing and localization: We identified thirteen group C alleles that disrupted only Rim101-dependent Snf7 function, including *snf7-6* and *snf7-48*. Because Snf7 interacts with Rim101 processing machinery, we predicted that alleles in this category would produce less active, processed Rim101, and that this decrease would explain the phenotypic defects observed

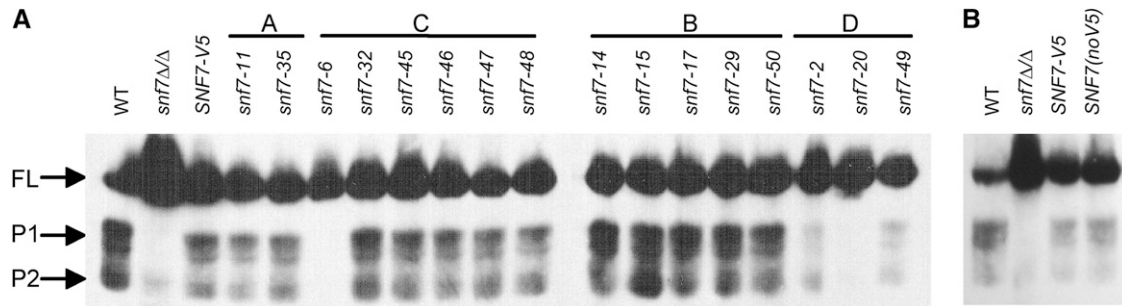


FIGURE 7.—(A) Rim101 processing is affected by some *snf7* mutants. Strains were grown to mid-log phase in M199 pH 8 medium before protein preparation. Equivalent protein amounts were analyzed by Western blotting analysis. FL, full length Rim101 (85 kDa); P1, processed form 1 of Rim101, the active form (74 kDa); P2, processed form 2 of Rim101, with unknown function (65 kDa). (B) Rim101 processing is decreased in the presence of only one *SNF7* allele regardless of V5 epitope.

in our screens. To test this prediction, we used Western blot analysis to investigate Rim101 processing in *snf7Δ/Δ RIM101-V5* strains containing mutant *snf7* alleles (Figure 7A). We noted that the *SNF7-V5* strain contained less processed Rim101 (both 74 and 65 kD forms) and more full-length Rim101 compared to wild-type cells. However, similar results were observed using an untagged *SNF7* complementation strain (Figure 7B), suggesting that decreased Rim101 processing in the *SNF7-V5* strain is not due to the V5 epitope.

We tested all *snf7* mutant alleles for their ability to promote Rim101 processing. As expected, all group A and group B alleles, such as *snf7-35* and *snf7-15* respectively, processed Rim101 similarly to the *SNF7-V5* strain. (Figure 7A). We expected group C alleles, which conferred only Rim101-dependent defects, to show decreased levels of Rim101 processing compared to the *SNF7-V5* strain. However, we found only one allele, *snf7-6*, that abolished Rim101 processing, similar to the *snf7Δ/Δ* strain (Figure 7A). Other group C alleles, such as *snf7-48*, processed levels of Rim101 similar to the *SNF7-V5* strain. We expected group D alleles, which conferred both ESCRT- and Rim101-dependent defects, to also have decreased levels of Rim101 processing compared to the *SNF7-V5* strain. This was observed for all group D alleles, including *snf7-20* (Figure 7A). Thus, while alleles in group B and group D behaved as expected, a decrease in processed Rim101 does not explain the growth defects seen in all group C alleles.

We considered two models to explain the processing seen in group C alleles. First, group C *snf7* alleles that process Rim101 do not promote translocation to the nucleus. Second, group C *snf7* alleles have Rim101 processing defects that were missed at steady-state growth. To test these models, we generated alanine-scanning *snf7* alleles without the V5 epitope and expressed them into a *snf7Δ/Δ RIM101-V5* strain. We grew our strains in acidic medium to mid-log phase and shifted them to alkaline medium for 30 min to investigate the initial stages of alkaline adaptation. We then tested Rim101 localization through immunofluorescence and Rim101 processing through Western blot analysis.

In a strain with wild-type *SNF7* grown at pH 4, Rim101-V5 showed cytoplasmic staining (data not shown). This same strain shifted to pH 8 showed V5 staining that colocalized with the DNA stain DAPI (Figure 8A), indicating nuclear localization of Rim101-V5 in these cells. The *snf7Δ/Δ* strain, which does not process Rim101, showed cytoplasmic V5 staining with no specific DAPI colocalization, indicating cytoplasmic retention of Rim101-V5 in this strain. We next analyzed the *snf7Δ/Δ* mutant complemented with wild-type *SNF7* or the group A allele *snf7-35.1*. As expected, strains containing either the wild-type *SNF7* allele or the *snf7-35.1* allele displayed wild-type Rim101-V5 staining patterns (Figure 8A), indicating nuclear localization of Rim101 in these strains. This correlates well with the robust processing promoted by these alleles (Figure 7A).

Next, we tested the group D alleles *snf7-20.1* and *snf7-49.1*. The *snf7-20.1* allele conferred severe growth defects (Figure 3) and contained no processed, active Rim101 (Figure 7). Cells expressing *snf7-20* displayed a V5 staining pattern similar to the *snf7Δ/Δ* strain, with no DAPI colocalization, indicating non-nuclear localization in these cells. The *snf7-49* allele conferred intermediate growth defects (Figure 3) and decreased active Rim101 (Figure 7). Cells expressing *snf7-49.1* displayed an intermediate V5 staining pattern with both DAPI-overlapping and non-DAPI overlapping staining (Figure 8A). This indicated partial nuclear localization and partial cytoplasmic retention of Rim101 in this strain. Thus, the Rim101-V5 localization in these group D strains correlated with the growth phenotype and Rim101 processing observed.

We then tested the group C alleles *snf7-47.1* and *snf7-48.1* that conferred Rim101-dependent defects yet had normal Rim101 processing (Figures 3 and 7 and data not shown). Strains expressing either of these alleles displayed strong cytoplasmic V5 compared with *snf7-35.1* and wild-type *SNF7* strains. While some cells showed slight V5 colocalization with DAPI, all cells maintained cytoplasmic staining (Figure 8A). We noted a stronger cytoplasmic staining pattern in the *snf7-48.1* strain compared to the *snf7-47.1* strain, which correlated with the slight difference in Rim101-dependent phenotypic

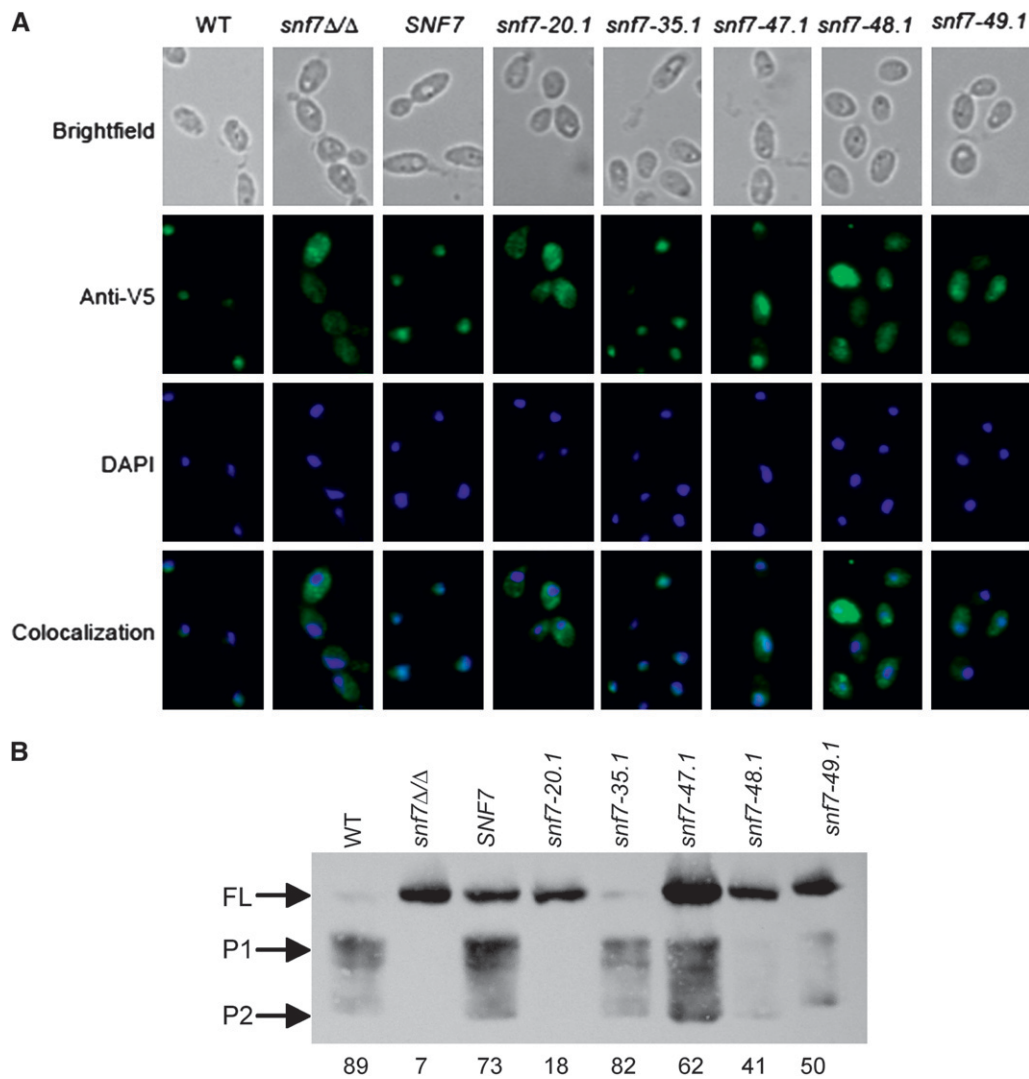


FIGURE 8.—(A) Rim101 localization in group C alleles may be impaired after a shift to alkaline pH. Strains were grown to mid-log phase in M199 (pH 4) medium and shifted to pH 8 for 30 min. Strains were fixed with 4% formaldehyde, spheroplasted, and attached to polylysine-treated wells for immunofluorescence. Samples were treated with anti-V5 antibody, followed by anti-mouse-IgG-alexafluor 488 (green). Nuclei were visualized by DAPI staining (blue). Strains investigated include *SNF7*^{+/+} *RIM101-V5* (WT) (DAY1212), *snf7* Δ/Δ *RIM101-V5* (DAY1127), *snf7* Δ/Δ *SNF7* *RIM101-V5* (DAY1128), *snf7* Δ/Δ *snf7-20.1* *RIM101-V5* (DAY1148), *snf7* Δ/Δ *snf7-35.1* *RIM101-V5* (DAY1149), *snf7* Δ/Δ *snf7-47.1* *RIM101-V5* (DAY1213), *snf7* Δ/Δ *snf7-48.1* *RIM101-V5* (DAY1150), and *snf7* Δ/Δ *snf7-49.1* *RIM101-V5* (DAY1214). (B) Rim101 processing in group C alleles may be impaired after a shift to alkaline pH. Strains were grown as in A before protein preparation. Equivalent protein amounts were analyzed by Western blotting analysis. Numbers under each column represent percentage P1 signal over total Rim101 (FL + P1 + P2) signal.

defects observed between these strains (data not shown). This indicates partial nuclear localization and partial cytoplasmic retention of Rim101-V5 in the *snf7-47.1* and *snf7-48.1* strains.

To determine how Rim101 processing is affected during adaptation to alkaline pH by these *snf7* alleles, we also examined Rim101 processing following a 30 min shift to alkaline pH. As previously observed (Figure 7), the wild-type strain processed Rim101-V5 and the *snf7* Δ/Δ strain did not (Figure 8B). Also, addition of *SNF7* or the group A *snf7-35.1* allele restored processing. Both group D alleles, *snf7-20.1* and *snf7-49.1*, conferred processing defects. Thus, these alleles promoted similar Rim101 processing under steady state and adaptive growth conditions.

However, we found that the group C allele *snf7-48.1* had considerably less Rim101-V5 processing than wild-type after a 30-minute shift to pH 8 compared to wild-type cells or compared to steady state growth at pH 8 (Figure 8B). This suggests that processing occurs more slowly in a *snf7-48* strain, but active Rim101 levels

eventually reach wild-type levels. We observed more processed Rim101 in the *snf7-47.1* strain, but noted that this strain still had less processed Rim101 (P1 + P2) relative to the amount of total Rim101 (FL + P1 + P2) than the control (Figure 8B). When we tested our 13 group C alleles, we observed a decrease in processed Rim101 relative to total Rim101 in 7 of 13 group C alleles (unpublished data). Taken together, these data suggest that many group C alleles, including *snf7-48*, fail to process Rim101 at the same rate as wild-type, but that Rim101-dependent phenotypic defects become less pronounced as processed Rim101 accumulates in the cell during steady-state growth.

Epithelial cell damage: *C. albicans* causes epithelial cell damage, and this damage requires active Rim101 (VILLAR *et al.* 2007; NOBILE *et al.* 2008). We wished to test the ability of our mutant *snf7* alleles to mediate epithelial cell damage in a Rim101-dependent and Rim101-independent manner. To do this, we utilized a radiolabeled FaDu oropharyngeal epithelial cell line.

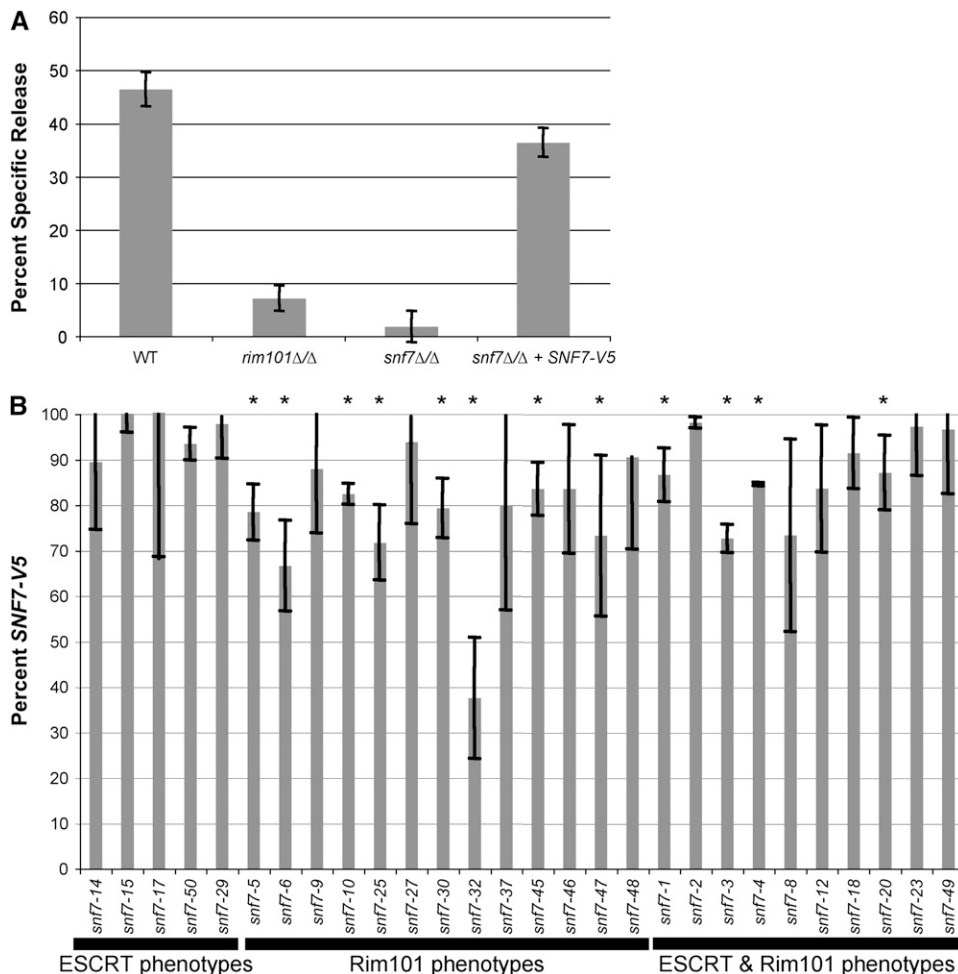


FIGURE 9.—*C. albicans*-mediated FaDu cell damage is affected by Rim101-dependent defects. (A) Both the *rim101Δ/Δ* mutant and *snf7Δ/Δ* mutant have severe FaDu cell damage defects, and the *SNF7-V5* allele rescues most of the *snf7Δ/Δ* defect. FaDu monolayers were Cr^{51} labeled overnight, then washed and incubated with 1×10^5 cells/ml *C. albicans* for 10 hr. Strains were tested in triplicate during each assay and compared with media-alone wells to measure specific Cr^{51} release. The assay was repeated at least three times; the figure denotes one representative assay. (B) Only mutant *snf7* alleles with Rim101-dependent defects have damage defects. Assays were run as described in A, and mutant *snf7* allele damage was compared to *SNF7-V5* damage. Each strain was tested in triplicate during each assay, and assays were repeated twice for each mutant *snf7* allele.

When incubated with the wild-type *C. albicans* strain, we observed ~45% specific release (Figure 9A). We observed significantly less damage when FaDu were incubated with the *rim101Δ/Δ* or *snf7Δ/Δ* strains. The addition of the *SNF7-V5* allele rescued most, but not all, of the damage defect in the *snf7Δ/Δ* strain (Figure 9A). Because the mutant *snf7* alleles were generated in the *SNF7-V5* background, we measured epithelial damage mediated by these mutant alleles and compared it to damage mediated by *SNF7-V5*.

We predicted that the group C alleles, which conferred only Rim101-dependent defects, would cause decreased epithelial cell damage due to their Rim101-related phenotypes. We tested thirteen group C alleles, of which eight caused less damage than the *SNF7-V5* allele ($p < 0.05$) (Figure 9B). We noted that *snf7-6*, the only group C allele to completely abolish Rim101 processing, did not have the strongest damage defect. In fact, none of the group C alleles were as diminished in damage as the *rim101Δ/Δ*, suggesting that all alleles maintained at least low levels of Rim101 activity. Overall, 62% of group C alleles caused less FaDu cell damage than the *SNF7-V5* allele.

Endocytosis plays an important role in receptor down-regulation and nutrient acquisition. We predicted that

full ESCRT function would be required for wild-type epithelial cell damage. However, because the group B allele growth and filamentation defects were less severe than the group C defects, we predicted the group B alleles would play a lesser role in epithelial cell damage than the group C alleles. In fact, we did not see a significant decrease in damage in any of the five alleles tested (Figure 9B). This suggests either that the ESCRT pathway does not contribute to FaDu cell damage or that the *snf7* alanine mutations do not abolish ESCRT function to levels that affect *C. albicans*-epithelial cell interactions.

Finally, we tested the group D alleles, which conferred both ESCRT- and Rim101-dependent defects. Four of ten group D alleles tested caused decreased FaDu damage ($p < 0.05$), and none of the defects were more severe than those conferred by the group C alleles (Figure 9B). Thus 40% of the group D alleles caused less damage than the *SNF7-V5* allele, likely due to Rim101-dependent defects.

DISCUSSION

Adaptation of *C. albicans* to a neutral-alkaline environment requires several cellular responses. One critical response is the activation of the transcription factor

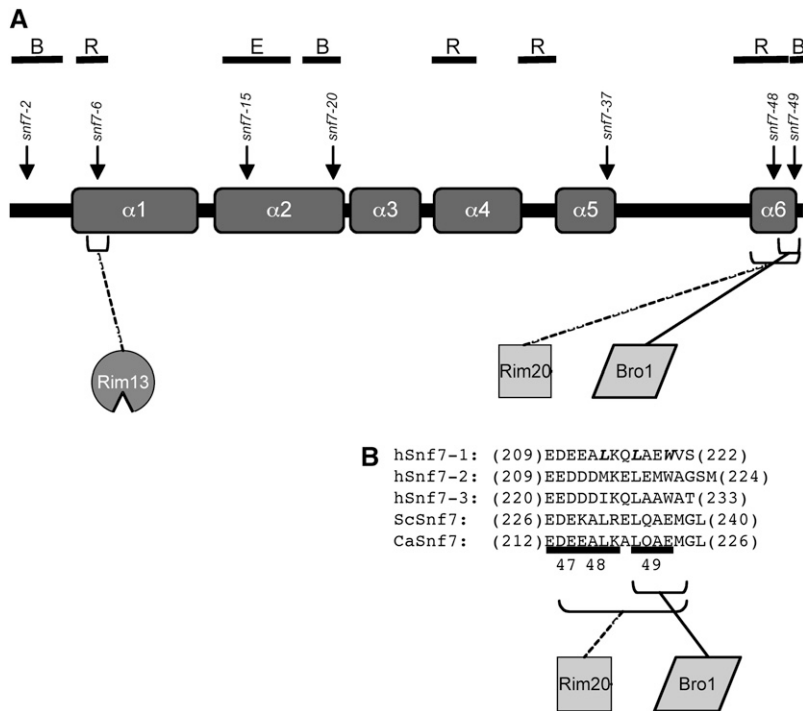


FIGURE 10.—Model of Snf7 interactions. (A) Snf7 interacts with ESCRT member Bro1, or Rim101 members Rim13 and Rim20, through distinct interaction domains. Putative Snf7 helical structure is shown with several *snf7* alleles marked for reference. Also noted are the domains predicted from our studies to be involved in ESCRT-specific (E), Rim101-specific (R), or both (B) processes. Solid lines represent interactions conserved in other species. Dashed lines represent interactions predicted from our data. (B) Alignment of Snf7 C-terminal sequence with *snf7* allele numbers noted below. Mutation of red residues abolished hSnf7-1–Bro1 domain interactions (McCULLOUGH *et al.* 2008). *C. albicans snf7* mutation of these residues has differential effect on bro1-domain protein interaction.

Rim101, which regulates gene expression in an extracellular pH-dependent manner. Another cellular change is the dependence on endocytosis and endosomal trafficking for uptake of otherwise inaccessible nutrients. Snf7 protein plays a pivotal role in both of these processes, and is therefore essential for the cellular adaptation to a neutral-alkaline environment. We investigated the role of Snf7 in these two distinct processes using alanine-scanning mutagenesis, which allowed us to examine the function of discrete regions of Snf7. Our analyses demonstrate that Snf7 function in the Rim101 pathway is separable from Snf7 function in the ESCRT pathway.

Separation of function and identification of functional domains: Our phenotypic results allowed us to characterize the mutant *snf7* alleles as nonfunctional, partially functional, or fully functional, with respect to the different phenotypic assays. To disrupt discrete domains, each mutation changed up to three amino acids. While we did not test Snf7 interactions directly due to the failure to generate functional tagged constructs, disruption of an interaction domain remains the simplest explanation for many of our partially complementary alleles.

The largest number of alleles (21) was classified into group A, the group of alleles conferring no defects or only one Rim101-dependent phenotypic defect. Of the 21 alleles included in this group, 19 have no apparent defect in any phenotypic assay tested. The largest cluster of group A alleles was a span of 25 amino acids in the C-terminal half of the protein. The J-Pred software program (CUFF and BARTON 2000) predicted six alpha-helices spanning the coding sequence (Figure 10),

which is similar to the predicted human Snf7 structures (SHIM *et al.* 2007). We aligned our phenotypic data with the predicted helical structures to correlate Snf7 structures and function. Interestingly, the cluster of group A alleles coincided with a region containing no predicted helices, suggesting that this lack of defined structure may increase tolerance for mutation in this region. The functional importance of the identified helices may explain their conservation through evolutionary time, while the less conserved unstructured regions suggest a linker sequence function.

We noted regions where adjacent alleles displayed similar phenotypic effects. There was one cluster of group D alleles at the N-terminus, indicating that this region of Snf7 is important for Rim101 and ESCRT functions. This region may function in Snf7 recruitment to the endosomal membrane through upstream interactions or it could be involved with a common downstream interaction. Because Snf7–bro1-domain interactions are the only common interactions yet identified between the *C. albicans* Rim101 and ESCRT pathways, and because Snf7–bro1-domain interactions have been mapped to the C-terminal end of Snf7 (see below), this region is more likely to be involved in upstream Snf7 function, such as recruitment by Vps20 or self-oligomerization. These alleles caused intermediate phenotypes, suggesting partial Snf7 activity, which may explain why we didn't observe differences in Snf7 localization (Figure 6 and data not shown).

The majority of group B alleles fell within the second predicted alpha helix, which spans residues 58–94 and encompasses *snf7-14* through *snf7-20*. CHMP3, the human Vps24 homolog, has a helical structure related

to CHMP4a, one of three human Snf7 homologs, and the second alpha helix of CHMP3 is important for self-interactions (MUZIOL *et al.* 2006; SHIM *et al.* 2007). We predict this region of Snf7 is important for an ESCRT-specific interaction, such as with the Vps2/Vps24 heterodimer or Vps4, which are necessary for endosomal trafficking but do not prevent Rim101 processing (XU *et al.* 2004). We demonstrated that Snf7-15 is able to cycle between endosome and cytoplasm by cell fractionation and immunofluorescence. These data indicate that Snf7-15 does not abolish Vps4 interactions. Failure of *snf7-14*, *snf7-15*, or *snf7-17* to efficiently self-oligomerize or to interact with downstream ESCRT-III members could account for the aberrant FM 4-64 trafficking seen in these strains (Figure 2), although the normal Snf7 protein localization pattern observed (Figure 6) indicates that minimally some Snf7 recycling occurs. Rim101-dependent growth and Rim101 processing appear normal in these strains, indicating that Rim101 activation is supported by the endosome-associated Snf7 present in these strains.

Strikingly, many group C alleles, which affect only Rim101-dependent phenotypes, cluster at the C-terminal alpha helix of Snf7. The clustering of group C alleles over this helix suggests that this structure may be specific for Snf7 interaction with Rim101 pathway proteins. Thus, this region of Snf7 is also a good candidate for interaction with a Rim101 pathway member, such as Rim13 or Rim20. The bro1-domain of the human Bro1 homolog (ALIX) was shown to interact with the C-terminal end of all three human Snf7 homologs, CHMP4a, 4b, and 4c (McCULLOUGH *et al.* 2008). The CHMP4 region important for ALIX interactions corresponds to the C-terminal group C cluster of *C. albicans* Snf7. This suggests the C-terminal region of Snf7 may be important for interactions with bro1-domain-containing proteins. However, we predicted that disrupting Snf7-bro1-domain interactions would affect both Rim101- and ESCRT-dependent phenotypes, which was only observed at the very C-terminal mutation, *snf7-49*. Why would mutations affecting interactions with one bro1-containing protein, Rim20, not affect interactions with another bro1-containing protein, Bro1? One possibility is that different bro1-containing proteins interact at this site using slightly different residues; residues changed in *snf7-48* may interrupt only Rim20 interactions, while those changed in *snf7-49* may interrupt both Rim20 and Bro1 interactions. This is supported by the fact that while all ALIX-CHMP4 interactions occurred at the C-terminal end of CHMP4, the critical residues for interaction varied between the three CHMP4 homologs (McCULLOUGH *et al.* 2008). Alternatively, the residues involved may be important for both Rim20 and Bro1 interactions, but the minor phenotypic defects of a failed Snf7-Bro1 interaction were not detected by our system for alleles other than *snf7-49*. The importance of this region for overall protein function is emphasized by

the failure of our C-terminally tagged Snf7 to fully complement a *snf7Δ/Δ* strain (data not shown). A third possibility is that the C-terminal group C cluster interacts with an unidentified Rim101 pathway member in *C. albicans*. In *A. nidulans*, *Yarrowia lipolytica*, and *S. cerevisiae*, an additional Rim101 pathway member, PalC/Rim23, has been identified which contains a bro1-domain and is able to interact with Snf7 (TILBURN *et al.* 2005; GALINDO *et al.* 2007; BLANCHIN-ROLAND *et al.* 2008). We identified *C. albicans* orf19.2914 through a blast search with ScRim23 sequence. If Orf19.2914 interacts with Snf7 through its bro1-domain, this interaction should occur at the Snf7 C-terminus, either in conjunction with Rim20 or on separate molecules of Snf7, which oligomerizes on the endosomal membrane.

Abnormal Snf7-Rim20 or Snf7-Rim13 interactions are possible explanations for group C phenotypes. However, it is possible that Rim13 interacts with a domain of Snf7 that also interacts with an ESCRT pathway member. A human homolog of Rim13, Calpain 7, was shown to interact with CHMP4b and CHMP4c through a microtubule interacting and trafficking (MIT) domain (SHIM *et al.* 2008). Vps4-ESCRT III member interactions also occur through a MIT domain at the N-terminus of Vps4 (SCOTT *et al.* 2005; TSANG *et al.* 2006). Calpain 7 contains two MIT domains, while Vps4 contains one. However, while the *A. nidulans* Rim13 homolog, PalB, has recently been shown to interact with an ESCRT-III member through an MIT domain, no MIT domains were identified in *S. cerevisiae* or *C. albicans* Rim13 (RODRIGUEZ-GALAN *et al.* 2008). While this does not rule out a shared Snf7-interaction domain between Rim13 and an ESCRT pathway member, it suggests that *C. albicans* Rim13 may interact with Snf7 in a manner not conserved among ESCRT pathway member interactions. Group C alleles, such as *snf7-6*, may affect these Rim13-Snf7 interactions.

Effects on Rim101 processing and regulation: Several mutant *snf7* alleles caused Rim101-dependent phenotypes without causing overt ESCRT-specific phenotypes (group C alleles). As described above, *snf7-6* may interrupt a domain necessary for Snf7 interactions with Rim101 processing machinery. We predict that the C terminus of Snf7 interacts with the bro1-domain of Rim20. Thus, we predict that *snf7-6* interrupts interaction with putative protease Rim13. Surprisingly, several C-terminal mutant alleles (*snf7-45*, *-46*, *-47*, and *-48*) showed Rim101-dependent defects but had Rim101 processing at levels comparable to the complemented strain during steady-state growth. We found that these strains have a Rim101 processing defect when shifted briefly to alkaline pH, indicating that these strains have a kinetic defect not observed during steady-state growth. Therefore, defective Rim101 processing accounts for all group C allele phenotypes.

Our phenotypic analyses, combined with structural and biochemical analyses, have allowed us to generate a model of Snf7 interactions (Figure 10). Our model

posits that after Snf7 has been recruited to the endosomal membrane, Snf7–Rim13 interactions occur at the region containing *snf7-6*, and that disruption of this region results in abrogation of Rim101 processing. Further, Snf7–Rim20 interactions occur at the C-terminal end, in a region spanning the area required for Snf7–Bro1 interactions. We can predict essential residues for Snf7–Bro1 domain interaction by aligning *C. albicans* Snf7 with *Homo sapiens* Snf7 proteins. McCULLOUGH *et al.* (2008) found three critical residues required for bro1-domain interaction with hSnf7-1 (Figure 10B). Our work suggests that these residues remain critical, but that Rim20–Snf7 interaction requires the entire sequence while Bro1–Snf7 interaction requires only the very C-terminal sequence. Rim20 and Bro1 colocalization has been observed under alkaline conditions (BOYSEN and MITCHELL 2006), suggesting that Rim101 processing and ESCRT function can occur simultaneously at the same Snf7 oligomerization site. Thus, under alkaline conditions, an undetermined factor, such as modified Rim8/PalF (HERRANZ *et al.* 2005), may promote Rim20–Snf7 interactions over Bro1–Snf7 interactions.

Effects on epithelial cell damage: Our data support the idea that Rim101 is necessary for wild-type levels of epithelial cell damage (Figure 9A). As we predicted, the majority of group C *snf7* alleles conferred reduced damage. We noted that the allele *snf7-6*, which abolished all Rim101 processing, caused more damage than the *rim101Δ/Δ* mutant. One explanation for this result is that the *snf7-6* allele processes very low levels of Rim101 undetectable by Western blot analysis. However, we favor the model that full-length Rim101 can mediate partial damage. This idea is supported in an endothelial cell damage model where a *rim8Δ/Δ* mutant caused less host cell damage than the *rim101Δ/Δ* mutant (DAVIS *et al.* 2000a). Further, the fact that the group C *snf7* alleles are not as deficient as the *snf7Δ/Δ* strain supports the idea that these alleles are at least partially functional.

We were surprised to find that group B alleles did not affect host cell damage in this model. MVB formation and vesicle trafficking are important for cell physiology. Several explanations may account for this observation. First, ESCRT function and MVB formation may not play an important role during epithelial cell damage. Epithelial cell damage depends on the ability of *C. albicans* to filament, and no group B allele affected filamentation as severely as the group C alleles. Second, ESCRT function may be important for acquiring nutrients, such as iron, for which the cells are not starved during the course of these assays. Third, the alleles may not fully knock down ESCRT function, as most *snf7* alleles affecting solely ESCRT function conferred intermediate FM 4-64 trafficking defects (Figure 2). Regardless, our data suggest that ESCRT function does not play a role during epithelial cell damage.

Effects on filamentation: Numerous redundant signals play a role in the regulation of filamentation,

including temperature, nutrient availability, and cell density. Defects in both vesicle trafficking and pH sensing have been shown to affect hyphal formation (DAVIS *et al.* 2000b; GUNTHER *et al.* 2005; PALMER *et al.* 2005; BERNARDO *et al.* 2008). Few of our alanine-scanning *snf7* alleles conferred strong defects in filamentation, which reinforces that few *snf7* alleles completely abolished Snf7 function. We were surprised to observe acidic filamentation of the *snf7Δ/Δ* and *vps4Δ/Δ* strains, suggesting that MVB trafficking may play an inhibitory function under acidic conditions. This was particularly remarkable as *snf7Δ/Δ* and *vps4Δ/Δ* strains have opposite effects on Rim101 processing: a *snf7Δ/Δ* strain is unable to process Rim101 and a *vps4Δ/Δ* strain constitutively processes Rim101 (KULLAS *et al.* 2004; HAYASHI *et al.* 2005). Although these null mutations have opposite effects on Rim101 processing, they have similar effects on ESCRT trafficking: both null mutations result in accumulation of endosomes unable to fuse with the vacuole. This suggests that aberrant ESCRT function results in acidic filamentation independent of Rim101 processing.

The intimate relationship between endocytosis and signal transduction has been established in various signaling pathways in many different organisms (POLO and DI FIORE 2006; KIRKIN and DIKIC 2007; VON ZASTROW and SORKIN 2007); however, much remains unknown regarding the exact nature of these relationships. Endocytosis can serve to downregulate receptors, to promote extended downstream signaling through “signaling endosomes,” or to generate physical proximity between members of a signaling pathway. The Rim101 pathway is likely a case of the latter model, with the signaling complex brought proximal to the processing complex to promote Rim101 processing. When Rim101 and ESCRT pathway members intersect remains unclear. The work done here demonstrates several functional regions of Snf7 that are specific for the Rim101 pathway, and suggests that bro1-domain containing proteins may interact at slightly divergent, though overlapping, Snf7 sites, leaving open the possibility that Rim13 and Rim20 interact with a single Snf7 monomer to facilitate Rim101 processing early in MVB formation.

Authors’ note: While this article was under review, a similar study was accepted investigating *S. cerevisiae* SNF7 (WEISS *et al.* 2009). WEISS *et al.* identified *snf7* alleles dysfunctional for MVB formation but functional for Rim101-dependent phenotypes. In agreement with our findings here, this study showed that *S. cerevisiae* SNF7 is also genetically separable, notably at the very N- and C-terminal ends, and that the phenotypes may be due to faulty Snf7–Vps4 interactions.

We thank members of the Davis lab for helpful discussion on this work and Lucia Zacchi and Dr. Kirsten Nielsen for critical review of the manuscript. We are grateful to Dr. Nielsen and Laura Okagaki for technical assistance with the microscopy. We are grateful to members

of the numerous groups in the *Candida* community involved in establishing an accessible genome database. This research of Dana A. Davis was supported in part by the Investigators in Pathogenesis of Infectious Disease Award from the Burroughs Wellcome Fund and by the National Institutes of Health (NIH) National Institute of Allergy and Infectious Disease award 1R01-AI064054-01 as well as T32DE007288 from the National Institute of Dental and Craniofacial Research. The content is solely the responsibility of the authors and does not necessarily represent the official views of the National Institute of Dental and Craniofacial Research or the National Institutes of Health.

LITERATURE CITED

- ADAMS, A., D. E. GOTTSCHLING, C. A. KAISER and T. STEARNS (Editors), 1997 *Methods in Yeast Genetics, 1997: A Cold Spring Harbor Laboratory Course Manual*. Cold Spring Harbor Laboratory Press, Cold Spring Harbor, NY.
- ANDRUTIS, K. A., P. J. RIGGLE, C. A. KUMAMOTO and S. TZIPORI, 2000 Intestinal lesions associated with disseminated candidiasis in an experimental animal model. *J. Clin. Microbiol.* **38**: 2317–2323.
- ARECHIGA-CARVAJAL, E. T., and J. RUIZ-HERRERA, 2005 The RIM101/pacC homologue from the basidiomycete *Ustilago maydis* is functional in multiple pH-sensitive phenomena. *Eukaryot. Cell* **4**: 999–1008.
- BABST, M., D. J. KATZMANN, E. J. ESTEPA-SABAL, T. MEERLOO and S. D. EMR, 2002a Escrt-III: an endosome-associated heterooligomeric protein complex required for mvb sorting. *Dev. Cell* **3**: 271–282.
- BABST, M., D. J. KATZMANN, W. B. SNYDER, B. WENDLAND and S. D. EMR, 2002b Endosome-associated complex, ESCRT-II, recruits transport machinery for protein sorting at the multivesicular body. *Dev. Cell* **3**: 283–289.
- BABST, M., B. WENDLAND, E. J. ESTEPA and S. D. EMR, 1998 The Vps4p AAA ATPase regulates membrane association of a Vps protein complex required for normal endosome function. *EMBO J.* **17**: 2982–2993.
- BAEK, Y. U., M. LI and D. A. DAVIS, 2008 *Candida albicans* ferric reductases are differentially regulated in response to distinct forms of iron limitation by the Rim101 and CBF transcription factors. *Eukaryot. Cell* **7**: 1168–1179.
- BENSEN, E. S., S. J. MARTIN, M. LI, J. BERMAN and D. A. DAVIS, 2004 Transcriptional profiling in *Candida albicans* reveals new adaptive responses to extracellular pH and functions for Rim101p. *Mol. Microbiol.* **54**: 1335–1351.
- BERNARDO, S. M., Z. KHALIQUE, J. KOT, J. K. JONES and S. A. LEE, 2008 *Candida albicans* VPS1 contributes to protease secretion, filamentation, and biofilm formation. *Fungal Genet. Biol.* **45**: 861–877.
- BILODEAU, P. S., J. L. URBANOWSKI, S. C. WINISTORFER and R. C. PIPER, 2002 The Vps27p Hse1p complex binds ubiquitin and mediates endosomal protein sorting. *Nat. Cell. Biol.* **4**: 534–539.
- BLANCHIN-ROLAND, S., G. DA COSTA and C. GAILLARDIN, 2008 Ambient pH signalling in the yeast *Yarrowia lipolytica* involves YIRim23p/PalC, which interacts with Snf7p/Vps32p, but does not require the long C terminus of YIRim9p/PalI. *Microbiology* **154**: 1668–1676.
- BORG-VON ZEPPELIN, M., S. BEGGAN, K. BOGGIAN, D. SANGLARD and M. MONOD, 1998 The expression of the secreted aspartyl proteinases Sap4 to Sap6 from *Candida albicans* in murine macrophages. *Mol. Microbiol.* **28**: 543–554.
- BOWERS, K., J. LOTTRIDGE, S. B. HELLIWELL, L. M. GOLDTHWAITE, J. P. LUZIO *et al.*, 2004 Protein–protein interactions of ESCRT complexes in the yeast *Saccharomyces cerevisiae*. *Traffic* **5**: 194–210.
- BOYSEN, J. H., and A. P. MITCHELL, 2006 Control of Bro1-domain protein Rim20 localization by external pH, ESCRT machinery, and the *Saccharomyces cerevisiae* Rim101 pathway. *Mol. Biol. Cell* **17**: 1344–1353.
- BRUCKMANN, A., W. KUNKEL, A. HARTL, R. WETZKER and R. ECK, 2000 A phosphatidylinositol 3-kinase of *Candida albicans* influences adhesion, filamentous growth and virulence. *Microbiology* **146**(11): 2755–2764.
- CUFF, J. A., and G. J. BARTON, 2000 Application of multiple sequence alignment profiles to improve protein secondary structure prediction. *Proteins* **40**: 502–511.
- DAVIS, D., 2003 Adaptation to environmental pH in *Candida albicans* and its relation to pathogenesis. *Curr. Genet.* **44**: 1–7.
- DAVIS, D., J. E. EDWARDS, JR., A. P. MITCHELL and A. S. IBRAHIM, 2000a *Candida albicans* RIM101 pH response pathway is required for host–pathogen interactions. *Infect. Immun.* **68**: 5953–5959.
- DAVIS, D., R. B. WILSON and A. P. MITCHELL, 2000b RIM101-dependent and-independent pathways govern pH responses in *Candida albicans*. *Mol. Cell. Biol.* **20**: 971–978.
- DAVIS, D. A., 2009 How human pathogenic fungi sense and adapt to pH: the link to virulence. *Curr. Opin. Microbiol.* **12**: 365–370.
- DAVIS, D. A., V. M. BRUNO, L. LOZA, S. G. FILLER and A. P. MITCHELL, 2002 *Candida albicans* Mds3p, a conserved regulator of pH responses and virulence identified through insertional mutagenesis. *Genetics* **162**: 1573–1581.
- FUJITA, H., M. YAMANAKA, K. IMAMURA, Y. TANAKA, A. NARA *et al.*, 2003 A dominant negative form of the AAA ATPase SKD1/VPS4 impairs membrane trafficking out of endosomal/lysosomal compartments: class E vps phenotype in mammalian cells. *J. Cell Sci.* **116**: 401–414.
- GALINDO, A., A. HERVAS-AGUILAR, O. RODRIGUEZ-GALAN, O. VINCENT, H. N. ARST, JR. *et al.*, 2007 PalC, one of two Bro1 domain proteins in the fungal pH signalling pathway, localizes to cortical structures and binds Vps32. *Traffic* **8**: 1346–1364.
- GIAEVER, G., A. M. CHU, L. NI, C. CONNELLY, L. RILES *et al.*, 2002 Functional profiling of the *Saccharomyces cerevisiae* genome. *Nature* **418**: 387–391.
- GOW, N. A., A. J. BROWN and F. C. ODDS, 2002 Fungal morphogenesis and host invasion. *Curr. Opin. Microbiol.* **5**: 366–371.
- GUNTHER, J., M. NGUYEN, A. HARTL, W. KUNKEL, P. F. ZIPFEL *et al.*, 2005 Generation and functional in vivo characterization of a lipid kinase defective phosphatidylinositol 3-kinase Vps34p of *Candida albicans*. *Microbiology* **151**: 81–89.
- HAYASHI, M., T. FUKUZAWA, H. SORIMACHI and T. MAEDA, 2005 Constitutive activation of the pH-responsive Rim101 pathway in yeast mutants defective in late steps of the MVB/ESCRT pathway. *Mol. Cell Biol.* **25**: 9478–9490.
- HERRANZ, S., J. M. RODRIGUEZ, H. J. BUSSINK, J. C. SANCHEZ-FERRERO, H. N. ARST, JR. *et al.*, 2005 Artrestin-related proteins mediate pH signaling in fungi. *Proc. Natl. Acad. Sci. USA* **102**: 12141–12146.
- HOWARD, D. H., 1999 Acquisition, transport, and storage of iron by pathogenic fungi. *Clin. Microbiol. Rev.* **12**: 394–404.
- ITO, T., T. CHIBA, R. OZAWA, M. YOSHIDA, M. HATTORI *et al.*, 2001 A comprehensive two-hybrid analysis to explore the yeast protein interactome. *Proc. Natl. Acad. Sci. USA* **98**: 4569–4574.
- KATZMANN, D. J., M. BABST and S. D. EMR, 2001 Ubiquitin-dependent sorting into the multivesicular body pathway requires the function of a conserved endosomal protein sorting complex, ESCRT-I. *Cell* **106**: 145–155.
- KATZMANN, D. J., C. J. STEFAN, M. BABST and S. D. EMR, 2003 Vps27 recruits ESCRT machinery to endosomes during MVB sorting. *J. Cell Biol.* **162**: 413–423.
- KIM, J., S. SITARAMAN, A. HIERRO, B. M. BEACH, G. ODORIZZI *et al.*, 2005 Structural basis for endosomal targeting by the Bro1 domain. *Dev. Cell* **8**: 937–947.
- KING, D. A., D. M. HANNUM, J. S. QI and J. K. HURST, 2004 HOCl-mediated cell death and metabolic dysfunction in the yeast *Saccharomyces cerevisiae*. *Arch. Biochem. Biophys.* **423**: 170–181.
- KIRKIN, V., and I. DIKIC, 2007 Role of ubiquitin- and Ubl-binding proteins in cell signaling. *Curr. Opin. Cell Biol.* **19**: 199–205.
- KRANZ, A., A. KINNER and R. KOLLING, 2001 A family of small coiled-coil-forming proteins functioning at the late endosome in yeast. *Mol. Biol. Cell* **12**: 711–723.
- KULLAS, A. L., M. LI and D. A. DAVIS, 2004 Snf7p, a component of the ESCRT-III protein complex, is an upstream member of the RIM101 pathway in *Candida albicans*. *Eukaryot. Cell* **3**: 1609–1618.
- KULLAS, A. L., S. J. MARTIN and D. DAVIS, 2007 Adaptation to environmental pH: integrating the Rim101 and calcineurin signal transduction pathways. *Mol. Microbiol.* **66**: 858–871.
- LAMBERT, M., S. BLANCHIN-ROLAND, F. LE LOUEDEC, A. LEPINGLE and C. GAILLARDIN, 1997 Genetic analysis of regulatory mutants

- affecting synthesis of extracellular proteinases in the yeast *Yarrowia lipolytica*: identification of a RIM101/pacC homolog. *Mol. Cell. Biol.* **17**: 3966–3976.
- LI, M., S. J. MARTIN, V. M. BRUNO, A. P. MITCHELL and D. A. DAVIS, 2004 *Candida albicans* Rim13p, a protease required for Rim101p processing at acidic and alkaline pHs. *Eukaryot. Cell* **3**: 741–751.
- LIU, H., 2001 Transcriptional control of dimorphism in *Candida albicans*. *Curr. Opin. Microbiol.* **4**: 728–735.
- LIU, H., 2002 Co-regulation of pathogenesis with dimorphism and phenotypic switching in *Candida albicans*, a commensal and a pathogen. *Int. J. Med. Microbiol.* **292**: 299–311.
- MAVOR, A. L., S. THEWES and B. HUBE, 2005 Systemic fungal infections caused by *Candida* species: epidemiology, infection process and virulence attributes. *Curr. Drug Targets* **6**: 863–874.
- MCCULLOUGH, J., R. D. FISHER, F. G. WHITBY, W. I. SUNDQUIST and C. P. HILL, 2008 ALIX-CHMP4 interactions in the human ESCRT pathway. *Proc. Natl. Acad. Sci. USA* **105**: 7687–7691.
- MITCHELL, B. M., T. G. WU, B. E. JACKSON and K. R. WILHELMUS, 2007 *Candida albicans* strain-dependent virulence and Rim13p-mediated filamentation in experimental keratomycosis. *Invest. Ophthalmol. Vis. Sci.* **48**: 774–780.
- MUHLRAD, D., R. HUNTER and R. PARKER, 1992 A rapid method for localized mutagenesis of yeast genes. *Yeast* **8**: 79–82.
- MUNN, A. L., and H. RIEZMAN, 1994 Endocytosis is required for the growth of vacuolar H(+)-ATPase-defective yeast: identification of six new END genes. *J. Cell Biol.* **127**: 373–386.
- MUZIOL, T., E. PINEDA-MOLINA, R. B. RAVELLI, A. ZAMBORLINI, Y. USAMI *et al.*, 2006 Structural basis for budding by the ESCRT-III factor CHMP3. *Dev. Cell* **10**: 821–830.
- NIKKO, E., and B. ANDRE, 2007 Split-ubiquitin two-hybrid assay to analyze protein–protein interactions at the endosome: application to *Saccharomyces cerevisiae* Bro1 interacting with ESCRT complexes, the Doa4 ubiquitin hydrolase, and the Rsp5 ubiquitin ligase. *Eukaryot. Cell* **6**: 1266–1277.
- NOBILE, C. J., N. SOLIS, C. L. MYERS, A. J. FAY, J. S. DENEULT *et al.*, 2008 *Candida albicans* transcription factor Rim101 mediates pathogenic interactions through cell wall functions. *Cell. Microbiol.* **10**: 2180–2196.
- ODORIZZI, G., D. J. KATZMANN, M. BABST, A. AUDHYA and S. D. EMR, 2003 Bro1 is an endosome-associated protein that functions in the MVB pathway in *Saccharomyces cerevisiae*. *J. Cell. Sci.* **116**: 1893–1903.
- OHSUMI, Y., and Y. ANRAKU, 1981 Active transport of basic amino acids driven by a proton motive force in vacuolar membrane vesicles of *Saccharomyces cerevisiae*. *J. Biol. Chem.* **256**: 2079–2082.
- OHSUMI, Y., and Y. ANRAKU, 1983 Calcium transport driven by a proton motive force in vacuolar membrane vesicles of *Saccharomyces cerevisiae*. *J. Biol. Chem.* **258**: 5614–5617.
- PALMER, G. E., M. N. KELLY and J. E. STURTEVANT, 2005 The *Candida albicans* vacuole is required for differentiation and efficient macrophage killing. *Eukaryot. Cell* **4**: 1677–1686.
- PENALVA, M. A., and H. N. ARST, JR., 2004 Recent advances in the characterization of ambient pH regulation of gene expression in filamentous fungi and yeasts. *Annu. Rev. Microbiol.* **58**: 425–451.
- PERLROTH, J., B. CHOI and B. SPELLBERG, 2007 Nosocomial fungal infections: epidemiology, diagnosis, and treatment. *Med. Mycol.* **45**: 321–346.
- PFALLER, M. A., and D. J. DIEKEMA, 2007 Epidemiology of invasive candidiasis: a persistent public health problem. *Clin. Microbiol. Rev.* **20**: 133–163.
- POLO, S., and P. P. DI FIORE, 2006 Endocytosis conducts the cell signaling orchestra. *Cell* **124**: 897–900.
- PORTA, A., A. M. RAMON and W. A. FONZI, 1999 PRR1, a homolog of *Aspergillus nidulans* palF, controls pH-dependent gene expression and filamentation in *Candida albicans*. *J. Bacteriol.* **181**: 7516–7523.
- RAMON, A. M., A. PORTA and W. A. FONZI, 1999 Effect of environmental pH on morphological development of *Candida albicans* is mediated via the PacC-related transcription factor encoded by PRR2. *J. Bacteriol.* **181**: 7524–7530.
- RODRIGUEZ-GALAN, O., A. GALINDO, A. HERVAS-AGUILAR, H. N. ARST and M. A. PENALVA, 2008 Physiological involvement in pH signaling of Vps24-mediated recruitment of *Aspergillus* PalB cysteine protease to ESCRT-III. *J. Biol. Chem.* **284**: 4404–4412.
- SCOTT, A., J. GASPAR, M. D. STUCHELL-BRERETON, S. L. ALAM, J. J. SKALICKY *et al.*, 2005 Structure and ESCRT-III protein interactions of the MIT domain of human VPS4A. *Proc. Natl. Acad. Sci. USA* **102**: 13813–13818.
- SHETH, C. C., E. G. MOGENSEN, M. S. FU, I. C. BLOMFIELD and F. A. MUHLSCHLEGEL, 2008 *Candida albicans* HSP12 is co-regulated by physiological CO₂ and pH. *Fungal. Genet. Biol.* **45**: 1075–1080.
- SHIM, S., L. A. KIMPLER and P. I. HANSON, 2007 Structure/function analysis of four core ESCRT-III proteins reveals common regulatory role for extreme C-terminal domain. *Traffic* **8**: 1068–1079.
- SHIM, S., S. A. MERRILL and P. I. HANSON, 2008 Novel Interactions of ESCRT-III with LIP5 and VPS4 and their implications for ESCRT-III disassembly. *Mol. Biol. Cell* **19**: 2661–2672.
- SIKORSKI, R. S., and P. HIETER, 1989 A system of shuttle vectors and yeast host strains designed for efficient manipulation of DNA in *Saccharomyces cerevisiae*. *Genetics* **122**: 19–27.
- SOUTHERN, P., J. HORBUL, D. MAHER and D. A. DAVIS, 2008 *C. albicans* colonization of human mucosal surfaces. *PLoS ONE* **3**: e2067.
- SPREGHINI, E., D. A. DAVIS, R. SUBARAN, M. KIM and A. P. MITCHELL, 2003 Roles of *Candida albicans* Dfg5p and Dcw1p cell surface proteins in growth and hypha formation. *Eukaryot. Cell* **2**: 746–755.
- TEIS, D., S. SAKSENA and S. D. EMR, 2008 Ordered assembly of the ESCRT-III complex on endosomes is required to sequester cargo during MVB formation. *Dev. Cell* **15**: 578–589.
- TILBURN, J., J. C. SANCHEZ-FERRERO, E. REYOY, H. N. ARST, JR. and M. A. PENALVA, 2005 Mutational analysis of the pH signal transduction component PalC of *Aspergillus nidulans* supports distant similarity to BRO1 domain family members. *Genetics* **171**: 393–401.
- TSANG, H. T., J. W. CONNELL, S. E. BROWN, A. THOMPSON, E. REID *et al.*, 2006 A systematic analysis of human CHMP protein interactions: additional MIT domain-containing proteins bind to multiple components of the human ESCRT III complex. *Genomics* **88**: 333–346.
- VIDA, T. A., and S. D. EMR, 1995 A new vital stain for visualizing vacuolar membrane dynamics and endocytosis in yeast. *J. Cell Biol.* **128**: 779–792.
- VILLAR, C. C., H. KASHLEVA, C. J. NOBILE, A. P. MITCHELL and A. DONGARI-BAGTZOGLOU, 2007 Mucosal tissue invasion by *Candida albicans* is associated with E-cadherin degradation, mediated by transcription factor Rim101p and protease Sap5p. *Infect. Immun.* **75**: 2126–2135.
- VINCENT, O., L. RAINBOW, J. TILBURN, H. N. ARST, JR. and M. A. PENALVA, 2003 YPXL/I is a protein interaction motif recognized by aspergillus PalA and its human homologue, AIP1/Alix. *Mol. Cell Biol.* **23**: 1647–1655.
- VON ZASTROW, M., and A. SORKIN, 2007 Signaling on the endocytic pathway. *Curr. Opin. Cell Biol.* **19**: 436–445.
- WEISS P., S. HUPPERT and R. KÖLLING, 2009 Analysis of the dual function of the ESCRT-III protein Snf7 in endocytic trafficking and in gene expression. *Biochem. J.* **424**: 89–97.
- WILLIAMS, R. L., and S. URBE, 2007 The emerging shape of the ESCRT machinery. *Nat. Rev. Mol. Cell Biol.* **8**: 355–368.
- WILSON, R. B., D. DAVIS and A. P. MITCHELL, 1999 Rapid hypothesis testing with *Candida albicans* through gene disruption with short homology regions. *J. Bacteriol.* **181**: 1868–1874.
- XU, W., and A. P. MITCHELL, 2001 Yeast PalA/AIP1/Alix homolog Rim20p associates with a PEST-like region and is required for its proteolytic cleavage. *J. Bacteriol.* **183**: 6917–6923.
- XU, W., F. J. SMITH, JR., R. SUBARAN and A. P. MITCHELL, 2004 Multivesicular body-ESCRT components function in pH response regulation in *Saccharomyces cerevisiae* and *Candida albicans*. *Mol. Biol. Cell* **15**: 5528–5537.
- YEO, S. C., L. XU, J. REN, V. J. BOULTON, M. D. WAGLE *et al.*, 2003 Vps20p and Vta1p interact with Vps4p and function in multivesicular body sorting and endosomal transport in *Saccharomyces cerevisiae*. *J. Cell Sci.* **116**: 3957–3970.

GENETICS

Supporting Information

<http://www.genetics.org/cgi/content/full/genetics.109.112029/DC1>

Mutational Analysis of *Candida albicans* SNF7 Reveals Genetically Separable Rim101 and ESCRT Functions and Demonstrates Divergence in bro1-Domain Protein Interactions

Julie M. Wolf and Dana A. Davis

Copyright © 2010 by the Genetics Society of America
DOI: 10.1534/genetics.109.112029

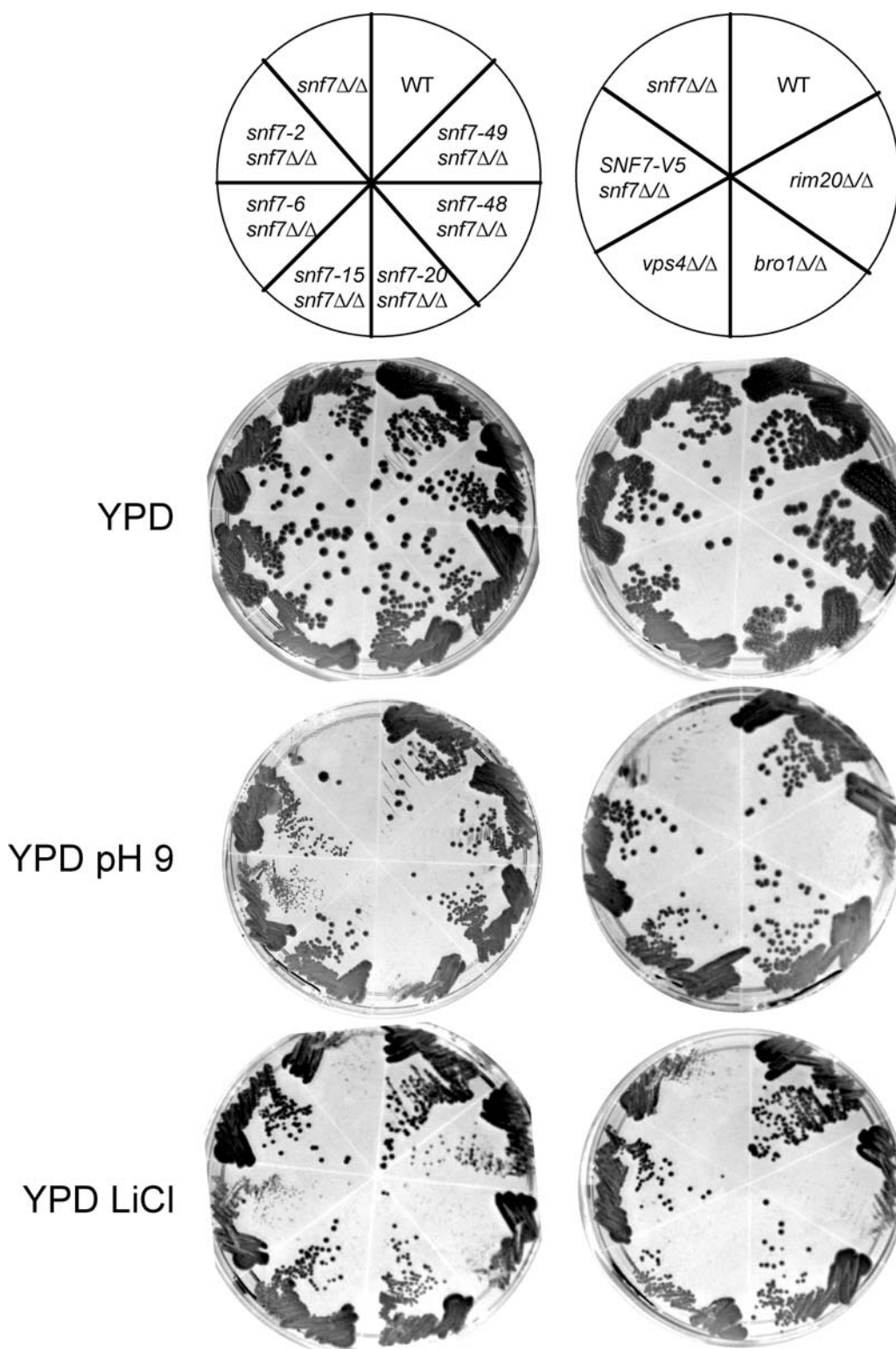


FIGURE S1.—Growth phenotypes of *snf7* mutants. Strains (identical to those used in Figure 3) include the wild-type (WT) (DAY185), *snf7* Δ/Δ (DAY763), *snf7* Δ/Δ + *SNF7-V5* (DAY980), *rim20* Δ/Δ (DAY1153), *bro1* Δ/Δ (DAY1156), *vps4* Δ/Δ (DAY1155), *snf7* Δ/Δ + *snf7-2* (DAY982), *snf7* Δ/Δ + *snf7-6* (DAY986), *snf7* Δ/Δ + *snf7-15* (DAY994), *snf7* Δ/Δ + *snf7-20* (DAY 999), *snf7* Δ/Δ + *snf7-48* (DAY1027), and *snf7* Δ/Δ + *snf7-49* (DAY1028). Strains were grown overnight at 30°C in YPD and streaked onto YPD, YPD pH 9, and YPD + LiCl for two days at 37°C prior to photographing.